

## N O T I C E

THIS DOCUMENT HAS BEEN REPRODUCED FROM  
MICROFICHE. ALTHOUGH IT IS RECOGNIZED THAT  
CERTAIN PORTIONS ARE ILLEGIBLE, IT IS BEING RELEASED  
IN THE INTEREST OF MAKING AVAILABLE AS MUCH  
INFORMATION AS POSSIBLE

**NASA CR-166720,**



**DEVELOPMENT OF THE COASTAL ZONE COLOR SCANNER FOR NIMBUS 7**

**VOLUME 1 - Mission Objectives and Instrument Description**

(NASA-CR-166720-Vol-1) DEVELOPMENT OF THE  
COASTAL ZONE COLOR SCANNER FOR NIMBUS 7.  
VOLUME 1: MISSION OBJECTIVES AND INSTRUMENT  
DESCRIPTION Final Report (Ball Aerospace  
Systems Div., Boulder) 76 p HC A05/MF A01

N82-11511

Unclass  
G3/43 01613

Ball Aerospace Systems Division  
P. O. Box 1062  
Boulder, CO 80306

May, 1979

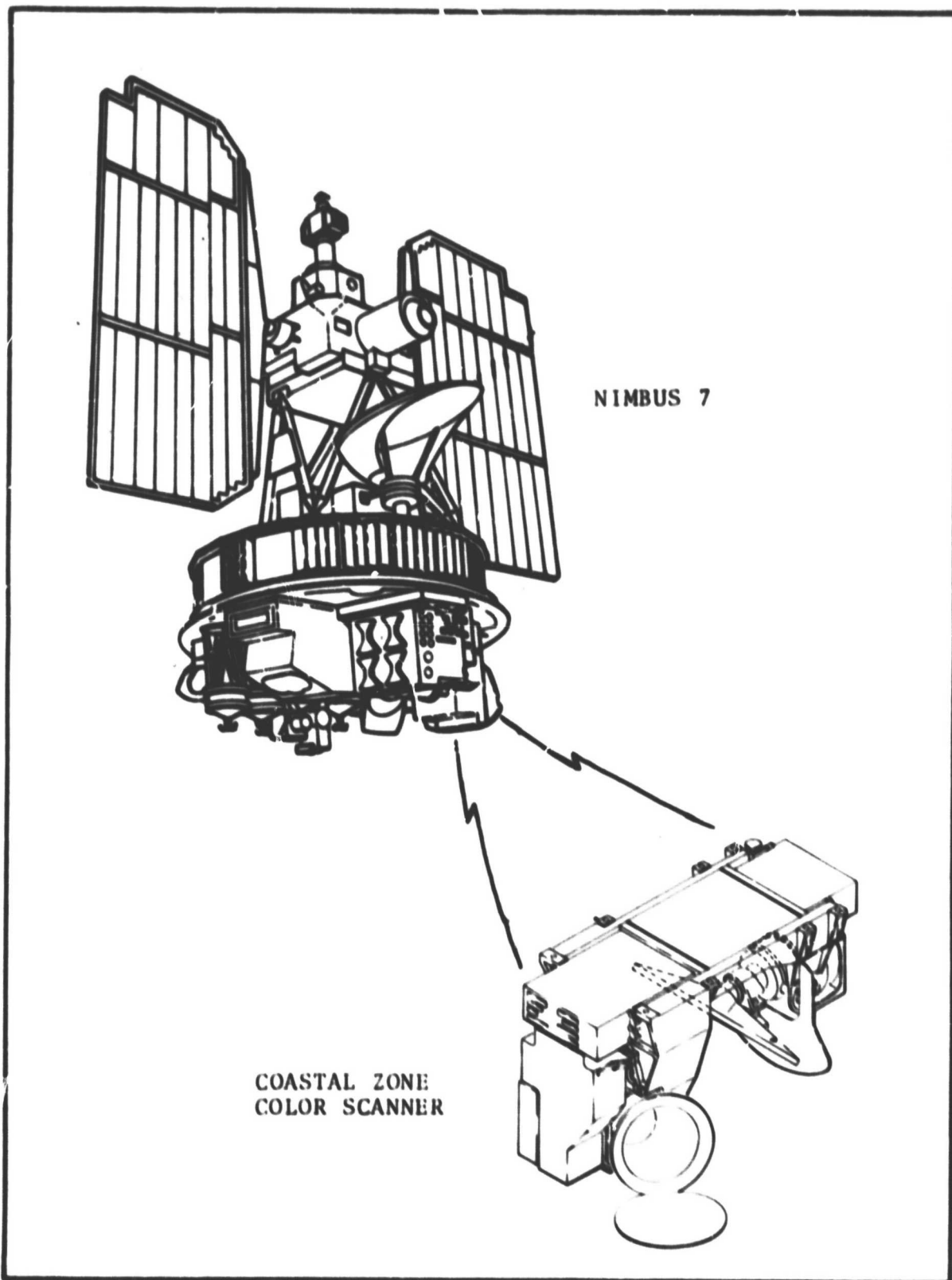
FINAL REPORT F78-11, Rev. A



Prepared For

NATIONAL AERONAUTICS AND SPACE ADMINISTRATION  
Goddard Space Flight Center  
Greenbelt, Maryland 29771

1. Report No. <b>F78-11, Rev. A</b>	2. Government Accession No.	3. Recipient's Catalog No.
4. Title and Subtitle <b>Development of the Coastal Zone Color Scanner for NIMBUS 7, Volume 1 - Mission Objectives and Instrument Description</b>	5. Report Date <b>May, 1979</b>	6. Performing Organization Code
	7. Author(s)	8. Performing Organization Report No.
9. Performing Organization Name and Address <b>Ball Aerospace Systems Division P.O. Box 1062 Boulder, CO 80306</b>	10. Work Unit No.	11. Contract or Grant No. <b>NAS5-20900</b>
	12. Sponsoring Agency Name and Address <b>National Aeronautics and Space Administration Goddard Space Flight Center Greenbelt, Maryland 20771</b>	13. Type of Report and Period Covered <b>Type III Final Report</b>
15. Supplementary Notes		
16. Abstract <p>This is the first of two volumes reporting on the development of the Coastal Zone Color Scanner for NIMBUS 7. This volume covers mission objectives, a system description, important or unique design features and a description of each subsystem.</p>		
17. Key Words (Selected by Author(s)) <b>Chlorophyll, phytoplankton, gelbstoffe, peaking preamplification, jitter, scanner</b>	18. Distribution Statement	
19. Security Classification (of this report)	20. Security Classification	21. No. of Pages 22. Price*





## Preface

The Coastal Zone Color Scanner (CZCS) is a 6-channel earth scanning radiometer for the measurement from orbit of chlorophyll and sediment in coastal waters. It was successfully launched on the NIMBUS 7 Spacecraft in October 1978. This Volume 1 of the final report covers an overview of the mission objectives, a description of the CZCS instrument, important design features, and details of the instrument's subsystems.



## TABLE OF CONTENTS

<u>Section</u>	<u>Title</u>	<u>Page</u>
	PREFACE	i
1	INTRODUCTION	1-1
2	MISSION OBJECTIVES AND INSTRUMENT DESCRIPTION	2-1
2.1	Mission Objectives	2-1
2.2	Instrument Description	2-1
3	IMPORTANT SYSTEM DESIGN FEATURES	3-1
3.1	Instantaneous Field-of-View and Co-Registration	3-1
3.2	Scan Field-of-View and Scan Rate	3-3
3.3	Spectral Response	3-7
3.4	Polarization Sensitivity	3-8
3.5	Scan Tilt	3-9
3.6	Signal to Noise Ratios & Noise Equivalent Temperature Difference	3-9
3.7	Commandable Gain and Threshold	3-10
3.8	Linearity of Response	3-11
3.9	Modulation Transfer Function	3-11
3.10	CZCS/Spacecraft Data Handling Interface	3-15
4	DESCRIPTION OF CZCS SUBSYSTEMS	4-1
4.1	Structure Subsystem	4-1
4.2	Optical Subsystem	4-1
4.3	Scanner Subsystem	4-11
4.4	Scan Electronics Subsystem	4-15
4.5	Analog Electronics Subsystem	4-20
4.6	Main Electronics Subsystem	4-25

## APPENDICES

<u>Appendix</u>	<u>Title</u>	<u>Page</u>
A	SCIENCE BACKGROUND	A-1



## TABLE OF CONTENTS (Continued)

## LIST OF ILLUSTRATIONS

<u>Figure</u>	<u>Title</u>	<u>Page</u>
2-1	Coastal Zone Color Scanner	2-1
2-2	Major Elements of the CZCS	2-3
2-3	Scan Geometry Provides Global Coverage	2-5
2-4	Optical Schematic	2-7
2-5	CZCS System Block Diagram	2-9
3-1	CZCS Scan Parameter Geometry	3-4
3-2	CZCS Data Window Organization (Per Channel)	3-5
3-3	CZCS Mirror Scan Positions	3-6
3-4	Video Channel 1 Through 4 Gain and Threshold	3-12
3-5	Channel 1-4 Thresholding Effect	3-13
3-6	Organization of CZCS Data by ZIP	3-18
4-1	CZCS Subsystem Interrelationship Block Diagram	4-2
4-2	CZCS Main Structure	4-3
4-3	Optical Arrangement	4-5
4-4	Visible Calibration Optics	4-6
4-5	Spectrometer Assembly	4-8
4-6	Channel 6 Optics	4-10
4-7	Scanner Subsystem	4-12
4-8	Scan Tilt Implementation	4-14
4-9	Scan Electronics Box	4-16
4-10	Scan Electronics Subsystem Assembled	4-18
4-11	Scan Drive/Momentum Compensator Functional Block Diagram	4-19
4-12	Analog Electronics Box	4-21
4-13	Typical Analog Electronics Circuit Board	4-22
4-14	Peaking Preamplification	4-23
4-15	Main Electronics Box	4-26
4-16	Power Supply Assembly	4-27
4-17	Main Electronics Box Assembled	4-28



## TABLE OF CONTENTS (Continued)

<u>Figure</u>	<u>Title</u>	<u>Page</u>
A-1	Laboratory Measured Reflectance of Chlorella	A-2
A-2	Atmospheric & Illumination Effects Involved in Establishing the Exposure of a Body of Water	A-3
A-3	Lear Jet Spectra at High and Low Altitudes	A-4
A-4	Ratios of Selected Wavelengths and Ground Truth vs. Position	A-6
A-5	High Altitude Spectra for Two Chlorophyll Concentrations	A-7
A-6	Calculated vs. Measured Chlorophyll Concentration, Gulf of Mexico	A-9
A-7	Chlorophyll & Temperature Correlation in Howe Sound British Columbia, Canada on May 26, 1971	A-11

<u>Table</u>	<u>Title</u>	<u>Page</u>
2-1	Each Channel in CZCS Responds to a Different Wavelength/Color	2-4
2-2	Significant CZCS Characteristics	2-10
3-2	Spectral Response Characteristics, Channels 1-6	3-7
3-3	Polarization in Channels 1-4 at Three Tilt Angles	3-8
3-4	CZCS Channel MTF's at Two Spatial Frequencies	3-15
4-1	Scan Tilt Measurements	4-15
4-2	Signal to Noise Ratio at Maximum Scene Radiance for a 60° Solar Zenith Angle in Channels 1-5	4-24





## Section 1 INTRODUCTION

This is Volume 1 of the final report for the Coastal Zone Color Scanner (CZCS), the first satellite-based remote sensing system for the measurement of water color. This report covers the period from the start of the hardware development in January, 1975 through the successful launch of NIMBUS 7 in October, 1978. It covers the design, assembly, and test of the CZCS Protoflight Model. The development of this model included design, breadboard and engineering model phases which led up to the assembly and test of the Protoflight Model. The results of the previous phases of work are reflected in the design and test results included in this report.

Volume 1 of this final report covers the following topics:

- A brief description of the CZCS mission objectives and an overview of the instrument developed to meet the mission objectives. This section is less technical in nature than the remaining sections.
- Important system design features are described.
- Design details and test results for each subsystem are covered.
- Appendix A presents additional science background related to the mission objectives.

Volume 2 of this final report covers the following topics:

- Prelaunch test results
- In-orbit performance data



## Section 2

### MISSION OBJECTIVES AND INSTRUMENT DESCRIPTION

The specifications imposed upon the hardware and the ultimate performance of the CZCS were driven by the science objectives of the mission. These objectives and a system description of the CZCS are covered in the following paragraphs.

#### 2.1 MISSION OBJECTIVES

The purpose of the CZCS project is to measure the abundance or density of chlorophyll at or near the sea surface in coastal waters. This will reveal the abundance of phytoplankton or planktonic plants which contain chlorophyll and are at the bottom of the oceanic food chain. Planktonic plants are the food of minute planktonic animals (zooplankton) which in their turn form the chief food supply of young fish. As the plankton drift with the sea currents, their location and that of the fish that feed on them is not static. The CZCS maps the location and measures the density of the plankton on a temporal or time scale, providing information to marine biologists and the fishing industry.

Additional objectives of the CZCS are the measurement of sediment or gelbstoffe (yellow stuff) in coastal waters, detection of surface vegetation, and the measurement of sea surface temperature. The temperature measurements can detect cold water upwelling which frequently provide the nutrient necessary for plankton "blooms" and can provide improved mapping of sea ice on a global scale.

Data will be available to investigators around the world as black and white photographs and as computer compatible tapes.

#### 2.2 INSTRUMENT DESCRIPTION

The Coastal Zone Color Scanner, shown in Figure 2-1 and 2-2, is an earth scanning six channel (detector) radiometer using a classical Cassegrainian telescope and a Wadsworth-type grating spectrometer. All six detectors observe

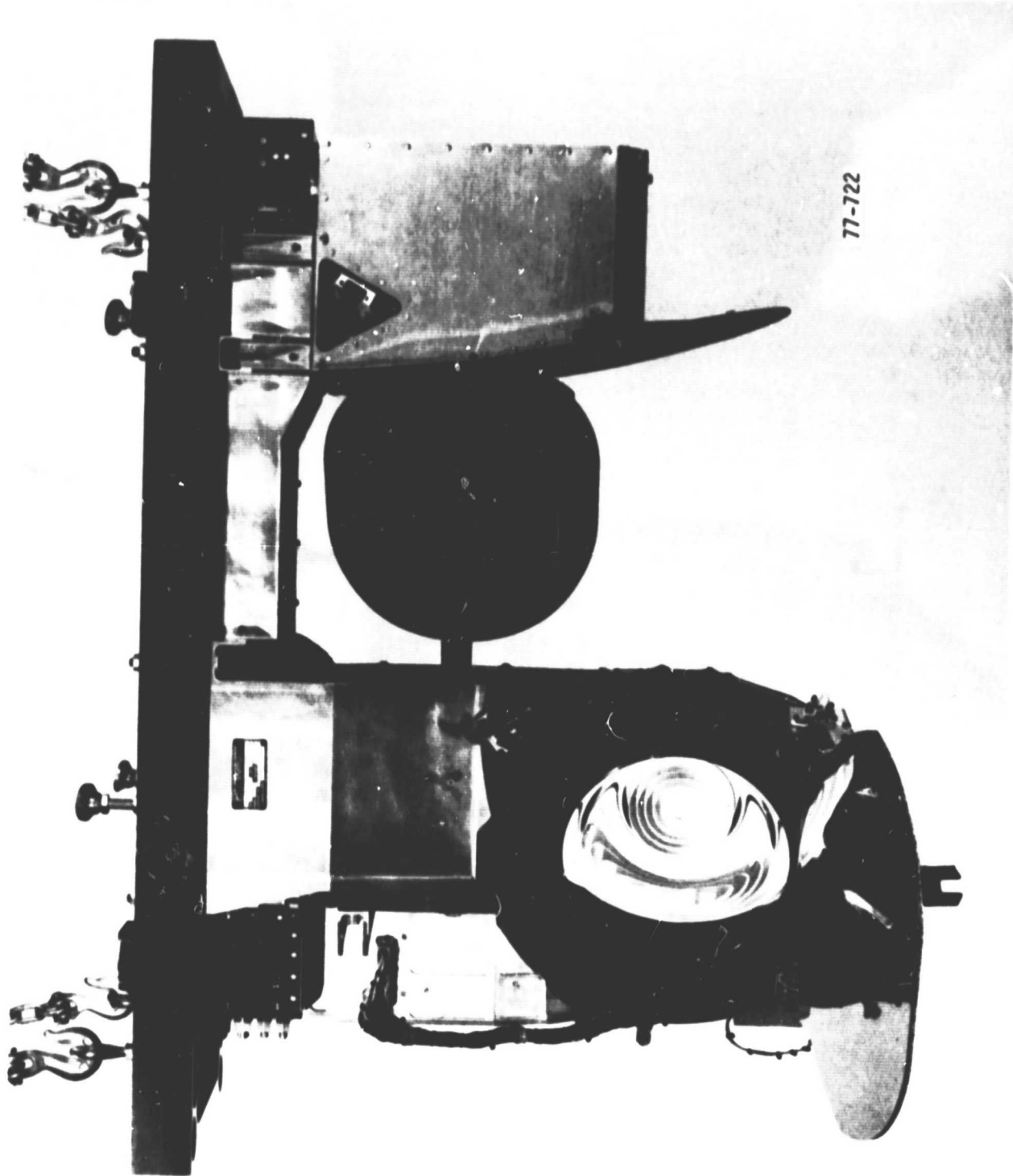


Figure 2-1 Coastal Zone Color Scanner

ORIGINAL PAGE IS  
OF POOR QUALITY

ORIGINAL PAGE IS  
OF POOR QUALITY

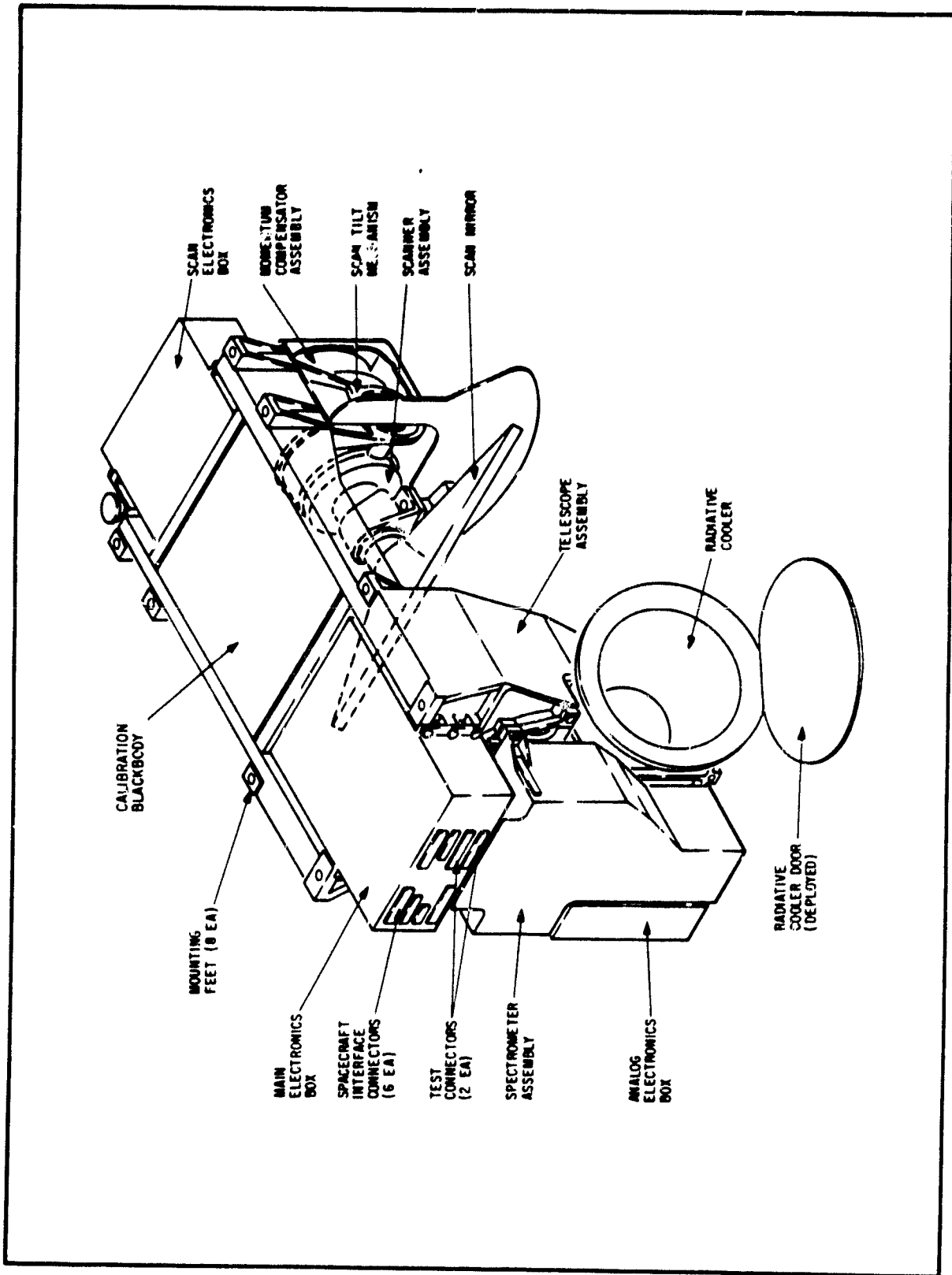


FIGURE 2-2 MAJOR ELEMENTS OF THE CZCS



the same area on the ground at the same time and differ only in the spectral range (or color) that they detect. The spectral ranges and functions are shown in Table 2-1.

Table 2-1  
EACH CHANNEL IN CZCS RESPONDS TO A DIFFERENT WAVELENGTH/COLOR

<u>Channel</u>	<u>Type</u>	<u>Spectral Range (<math>\mu\text{m}</math>)</u>	<u>Color</u>	<u>Function</u>
1	visible	0.433 - 0.453	purple	chlorophyll
2	visible	0.510 - 0.530	blue-green	reference
3	visible	0.540 - 0.560	yellow-green	sediments
4	visible	0.660 - 0.680	red	chlorophyll
5	Near IR	0.700 - 0.800	--	surface vegetation
6	IR	10.5 - 12.5	--	surface temperature

A continuously rotating mirror scans a nominal 0.865 mrad (0.05 degree) Instantaneous Field-Of-View (IFOV) across the earth's surface perpendicular to the orbit track at 8.08 revolutions per second. The spacecraft's orbital velocity provides the other scan direction. At the orbital attitude of 597 miles (955 km), this results in an instantaneous view of the earth's surface of 0.5 miles (0.8 km) square. An unobstructed scan angle of approximately  $\pm 40$  degrees on either side of nadir produces a scan width on the ground of 1000 miles (1600 km). Putting it another way, a single scan of the mirror provides a view of the earth 1000 miles long and one half mile wide. The spacecraft motion is such that successive scans are contiguous, resulting in a complete raster. The rotation of the earth under the spacecraft allows for total global coverage every twenty-four hours. Figure 2-3 illustrates the scan pattern.

The scan mirror is made of beryllium, plated with nickel, and coated with silver. The silver coating is protected from oxidation by a thin layer of quartz. The instrument has the capability of minimizing solar glint (which can distort the reflected water color) by tilting, upon command, the scan mirror about the telescope axis from its nominal 45 degrees. This results in the instrument field-of-view looking ahead or behind the spacecraft and away from

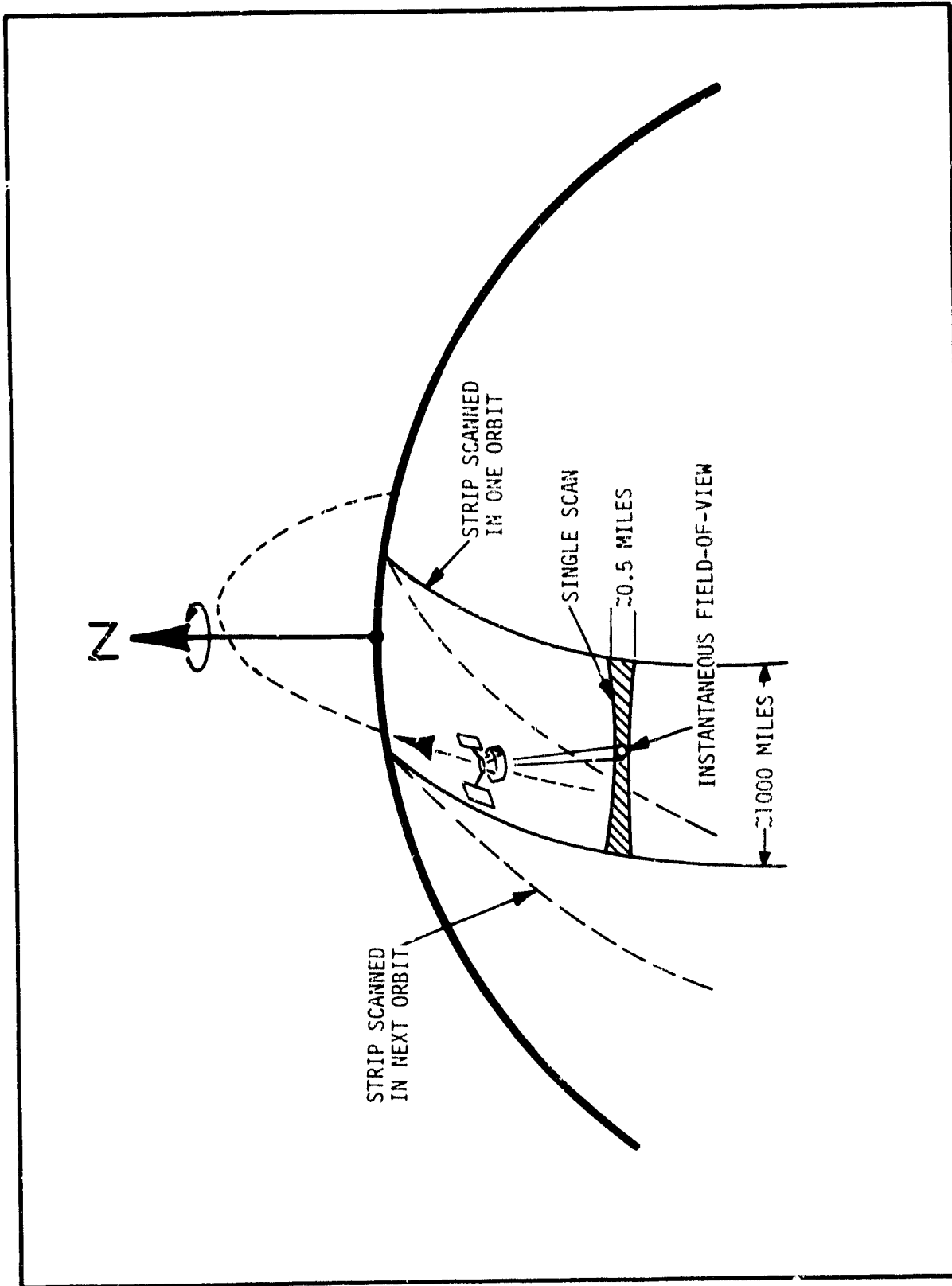


Figure 2-3 Scan Geometry Provides Global Coverage



the glint. The field-of-view tilt adjustments can be made in two degree increments over a range of  $\pm 20$  degrees from nadir.

Figure 2-4 illustrates the Optical System in the CZCS. Scan scenes are separated into two spectral ranges, the visible (and near infrared) and the infrared, by a dichroic beamsplitter and directed along separate paths. Radiance of the visible spectra is passed into the spectrometer where it passes through a two element depolarization wedge which "scrambles" any polarized radiance in the scene and corrects for polarization introduced by the scan mirror and other pre-optics. After folding by additional mirrors, the radiance is dispersed by the concave diffraction grating. Each of the five silicon photodiode detectors then senses a separate band of wavelengths or color. Coregistration of the five detectors is assured by the use of a single, common, field stop prior to the spectrometer.

The infrared radiance is reflected by the dichroic and directed through three lenses to a HgCdTe photoconductor detector. The detector size defines this channel's field-of-view and a unique coating on one of the lenses defines the spectral bandwidth. The detector is mounted to the inner stage or "patch" of a radiative cooler. Through radiative transfer, the detector is cooled to 120K ( $-243^{\circ}\text{F}$ ) with temperature control provided electronically. The door of the radiative cooler is opened during cooler operation and shields the cooler from a direct look at the earth.

An in-flight calibration package for the five visible detectors is located within the spectrometer. It consists of two (redundant) incandescent lamps, spectral shaping optics, and a motor driven shutter. The calibration beam is allowed to pass through a hole in the collimating mirror during the back scan of the scan mirror where it follows the normal light path to the grating and detectors.

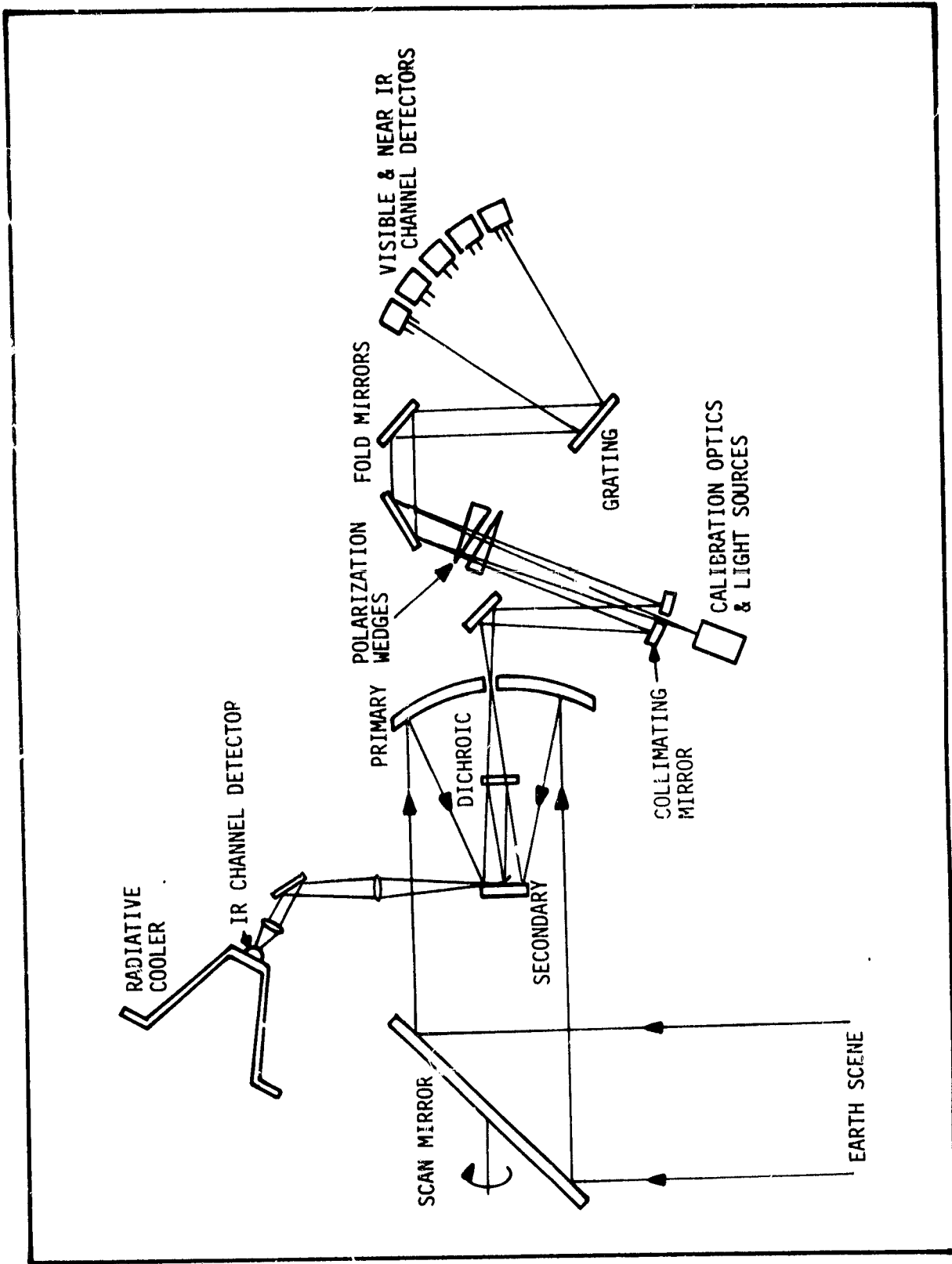


Figure 2-4 Optical Schematic





Calibration for the infrared detector is also provided during the backscan when the scan mirror views a honeycomb blackbody mounted to the instrument structure.

An additional look at the system operation is provided by Figure 2-5, the CZCS System Block Diagram. After analog signal conditioning, the video signals from each of the six channels are quantized by individual analog to digital converters with 8 bit or 255 level resolution. Sampling is performed every 13.75 microseconds concurrently in each channel. The 8 bit words for each channel are then sequenced consecutively to the CZCS Information Processor (ZIP) located in the spacecraft.

The system characteristics are summarized in Table 2-2.





Table 2-2  
SIGNIFICANT CZCS CHARACTERISTICS

WEIGHT:	93 lbs. (42 kg)
DIMENSIONS:	32 INCHES LONG (81 cm) 15 INCHES WIDE (38 cm) 22 INCHES HIGH (56 cm)
POWER:	50 WATTS (AVERAGE)
SCAN RATE:	8.08 RPS (485 RPM)
DATA SCAN:	$\pm 39.2^\circ$
SCAN TILT:	$\pm 20^\circ$ in $2^\circ$ INCREMENTS
SCAN JITTER:	1.8 MICROSECONDS (IN VACUUM)
INSTANTANEOUS FIELD-OF-VIEW	<0.865 mrad (CHANNELS 1-5) 0.927 x 0.88 mrad (CHANNEL 6)
MAXIMUM DATA RATE:	$3.5 \times 10^6$ BITS/SECOND
BUFFERED DATA RATE: (BY ZIP)	$8 \times 10^5$ BITS/SECOND
SAMPLING RATE:	$72.72 \times 10^3$ SAMPLES/SECOND
SAMPLING RESOLUTION:	8 BITS (PER CHANNEL)
SUBSATELLITE (NADIR) RESOLUTION: (AT ORBITAL ALTITUDE OF (955 Km)	<0.826 km (0.51 MILES) (CHANNELS 1-5) 0.885 x 0.84 km (0.55 x 0.53 miles) (CHANNEL 6)
DETECTORS:	SILICON PHOTODIODES (CHANNELS 1-5) HgCdTe PHOTOCONDUCTOR (CHANNEL 6)
DIAMETER OF OPTICAL APERTURE:	7 INCHES (17.8 cm)
FOCAL LENGTH OF CHANNELS 1-5:	28 INCHES (71.1 cm)
FOCAL LENGTH OF CHANNEL 6:	4.5 INCHES (11.4 cm)



### Section 3 IMPORTANT SYSTEM DESIGN FEATURES

The CZCS design contains many features of great importance to the success of the mission. These include:

- Instantaneous Field-of-View
- Co-Registration
- Scan Field-of-View
- Spectral Response
- Polarization Sensitivity
- Scan Tilt
- Signal-to-Noise Ratio
- Noise Equivalent Temperature Difference
- Gain and Threshold
- Linearity of Response
- Modulation Transfer Function
- Data Handling Interface

The significance of each of these features is discussed in the following sections. More design details can be found in Section 4.

#### 3.1 INSTANTANEOUS FIELD-OF-VIEW AND CO-REGISTRATION

The instantaneous field of view (IFOV) of an instrument like the CZCS is the divergence of the solid angle of acceptance of that instrument, and sets the ground resolution. Nadir or subsatellite resolution is  $H \tan \theta$  where  $H$  is the orbital altitude and  $\theta$  is the angular field-of-view.

It is important in the CZCS instrument that the IFOV of each of the six channels be the same size and be coregistered to one another. This is necessary so that all channels view the same area on the ground simultaneously.

The problem of IFOV size and coregistration in channels 1 through 5 is solved through the use of a single common field stop for these channels located prior



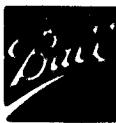
to the spectrometer in the optical path. The size of the field stop divided by the effective focal length (EFL) of the telescope sets the field of view for these channels. Since channels 1 through 5 all view this field stop, the IFOV's are equal and inherently "perfectly" coregistered.

For channel 6, the infrared channel, the detector itself is the field stop. The optical design allow for positional adjustment of two mirrors, a lens, and the radiative cooler to adjust the size of the channel 6 IFOV and to align it with the IFOV of the other channels.

Table 3-1 summarizes the IFOV's and registration of the six channels in the X-axis (perpendicular to the spacecraft velocity vector) and the Y-axis (parallel to the spacecraft velocity vector). The 0.08 mrad misregistration of Channel 6 is less than 1/10 of the IFOV. Measurements made after instrument vibration indicate no change in the coregistration demonstrating the effectiveness of the design. In Channel 1, the ground resolution for a 955 kilometer orbital altitude, calculated using the  $H \tan \theta$  relationship, is 778 by 774 meters or 0.483 by 0.476 statute miles. The misregistration is 76 meters or 250 feet.

Table 3-1  
MEASURED INSTANTANEOUS FIELD-OF-VIEW (IFOV) AND  
CO-REGISTRATION OF CZCS CHANNELS 1-6

<u>CHANNEL</u>	<u>X-AXIS</u>		<u>Y-AXIS</u>	
	<u>IFOV</u>	<u>Registration Error</u>	<u>IFOV</u>	<u>Registration Error</u>
1	0.815 mrad	0.02 mrad	0.81 mrad	0 mrad
2	0.815 mrad	0 mrad	0.785 mrad	0 mrad
3	0.810 mrad	0 mrad	0.795 mrad	0 mrad
4	0.830 mrad	0 mrad	0.810 mrad	0 mrad
5	0.825 mrad	0 mrad	0.805 mrad	0 mrad
6	0.927 mrad	0.08 mrad	0.880 mrad	0.08 mrad



### 3.2 SCAN FIELD-OF-VIEW AND SCAN RATE

The CZCS has an effective scan field-of-view of  $\pm 39.36^\circ$  or  $\pm 687$  milliradians. This is illustrated by Figure 3-1, Scan Parameter Geometry, which shows design guidelines of a  $\pm 700$  milliradian scan field-of-view, an IFOV of 0.865 mrad and the forward and aft tilt of  $\pm 350$  mrad. The latter is discussed in Section 3-5 of this report. The scan rate and the scan field of view are interrelated in that both are a function of the average data rate and the sampling rate. The scan period must be synchronous with the spacecraft clock and both the scan period and the scan field have to be synchronous with the sampling material, i.e., the total scan and the scan field should contain an integral number of samples.

The CZCS employs a fully rotating scan mirror. For near continuity at nadir, a scan period of 123.75 milliseconds, was selected. At the sampling period of 13.75 microseconds, we have 9,000 data sampling intervals per scan line. For the orbital altitude of 955 km and the nominal IFOV (see Figure 3-1) the overlap of resolution elements from scan line to scan line is four percent.

The CZCS Information Processor or "ZIP" has a capability of 800 kilobits per second. As some ZIP and spacecraft timing data is also included in that, the data rate for CZCS was arbitrarily set at  $7.9 \times 10^5$  bits per second for design purposes. The six CZCS channels are sampled every 13.75 microseconds with each channel digitized to eight bits. The maximum data rate is, therefore,  $3.491 \times 10^6$  bits per second for design purposes. Therefore, data samples are only taken during the active Earth scan of  $\pm 39.96^\circ$ , in-flight calibration targets in the backscan and multiplexed telemetry as illustrated in Figure 3-2. As shown, there are 2,040 active samples or pixels per scan; 1968 in the Earth scan, 64 for voltage calibration, 4 for housekeeping, and blackbody telemetry and 4 for in-flight radiance calibration. These values and the format were worked out in meetings with General Dynamics (the ZIP contractor), GSFC, and General Electric. The buffered data rate from the CZCS is 791,273 bits per second. The d.c. restorer interval data are not readout, but used internally by the CZCS. The nadir pixel or sample was measured to be 1,090 rather than the 1,098 shown on Figure 3-3. This means that the scan is skewed

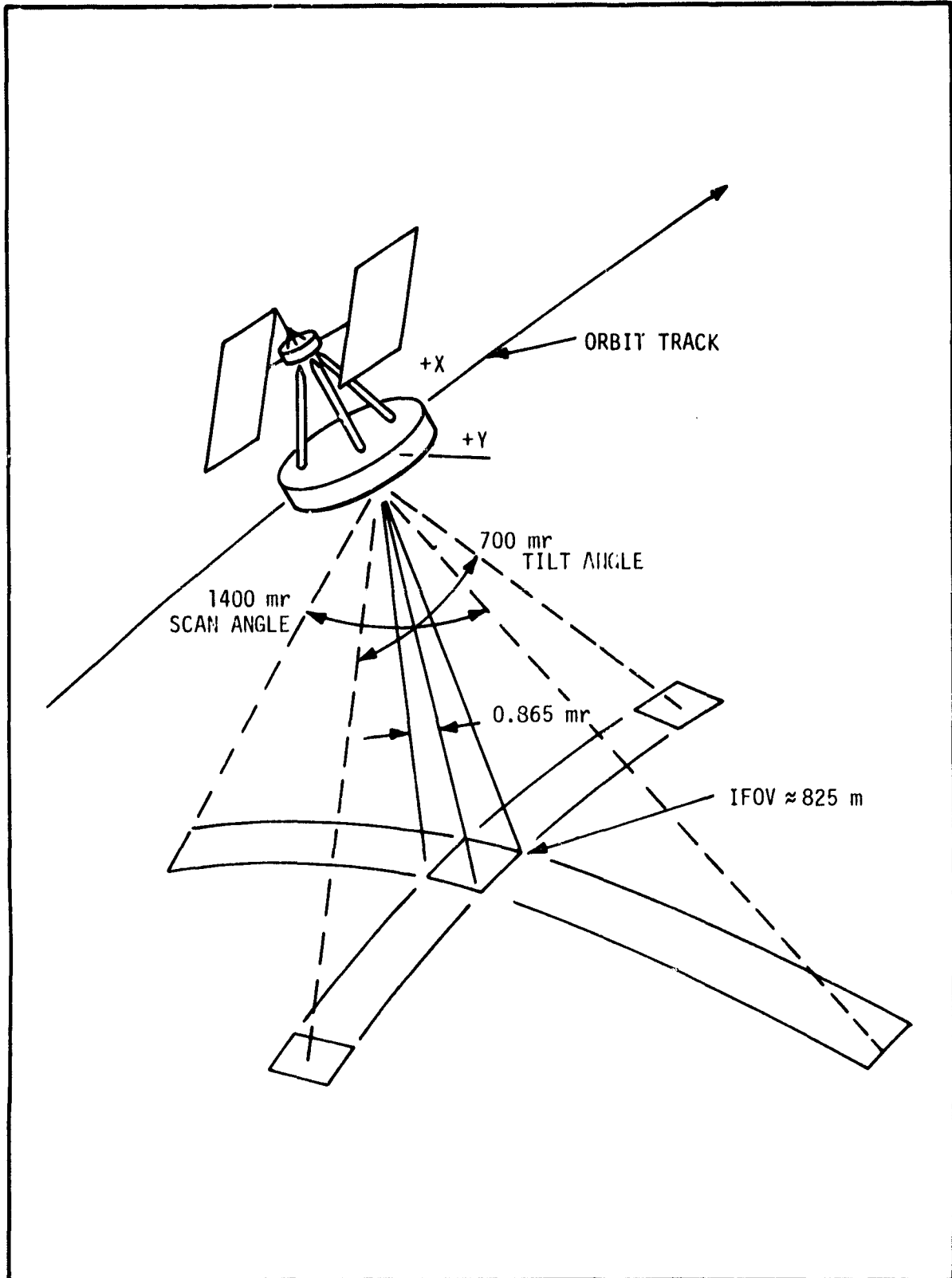


FIGURE 3-1 CZCS SCAN PARAMETER GEOMETRY

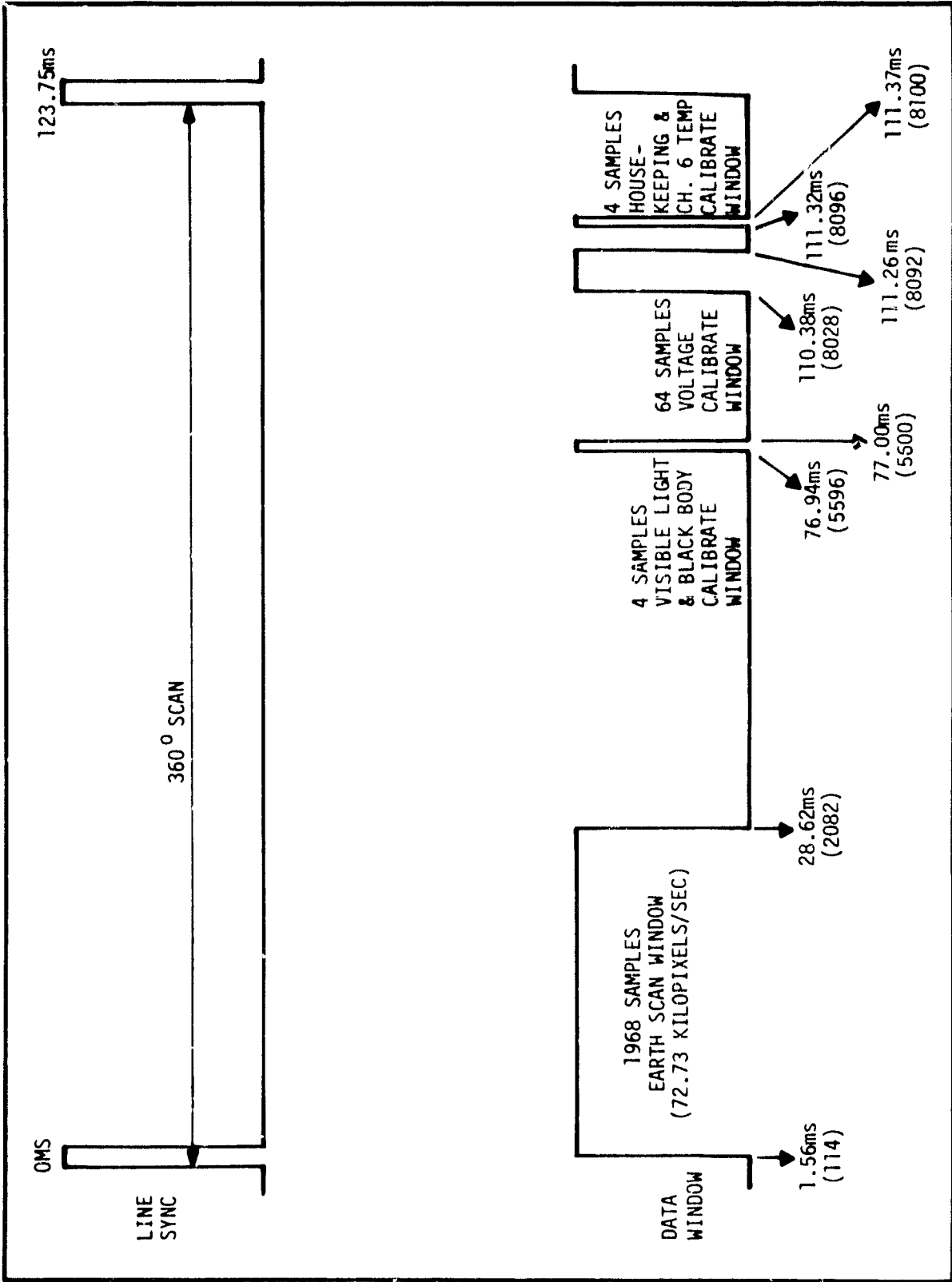


Figure 3-2 CZCS Data Window Organization (Per Channel)



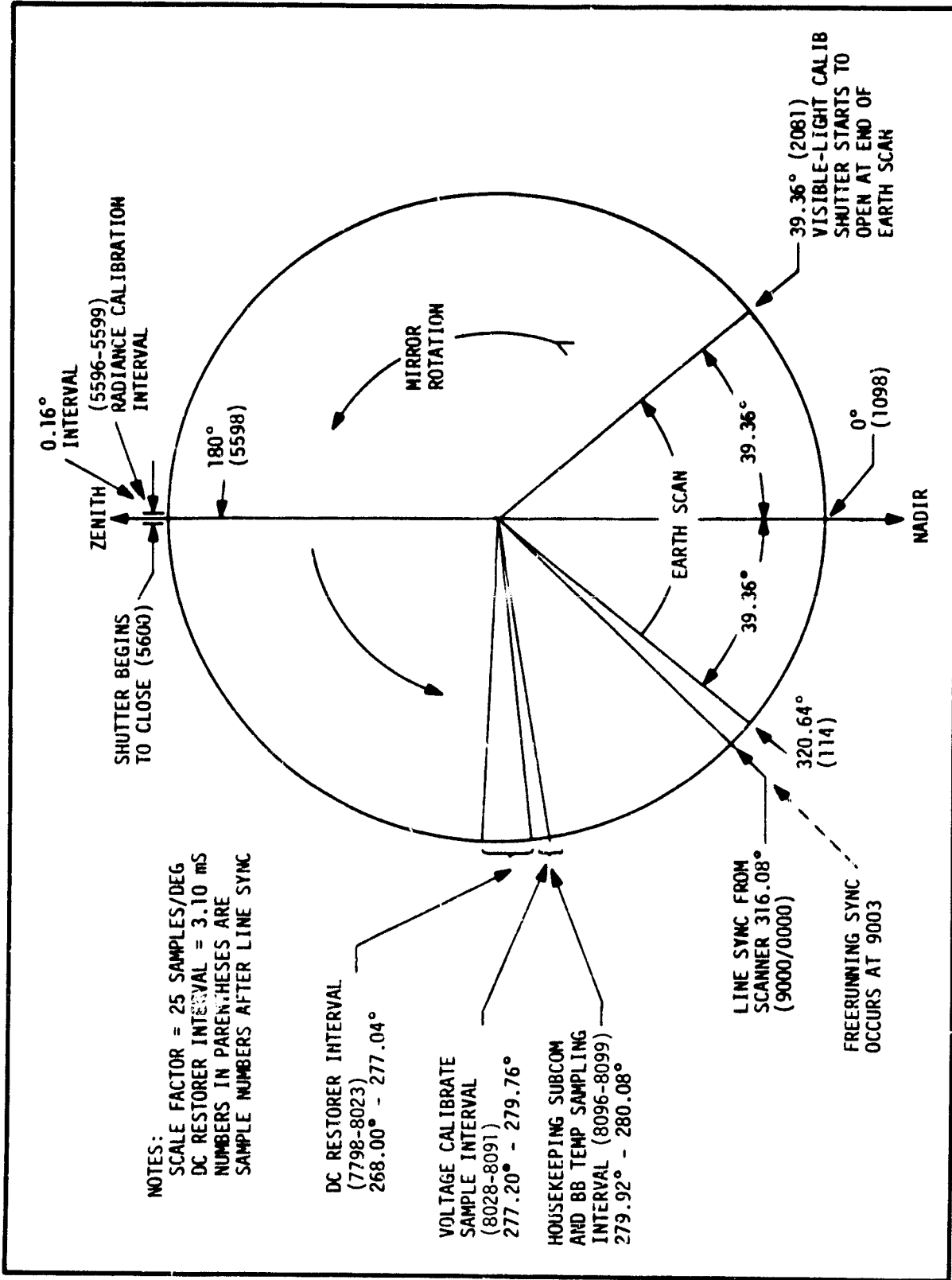


Figure 3-3 CZCS MIRROR SCAN POSITIONS



by 0.32° in the direction of space and extends from 39.68° on the space side to 39.04° on the satellite side.

### 3.3 SPECTRAL RESPONSE

The spectral response of all six channels are critical to the science of the instrument (see Appendix A of this volume for details). The spectral responses for channels 1 through 5 are determined by individual exit slits in the spectrometer focal plane in front of each detector and field lens. Electron discharge milling (EDM) of the exit slits was necessary to achieve the close mechanical (and hence spectral bandpass) tolerances. Each slit was also mechanically adjustable in order to select the proper spectral center point.

The spectral bandpass for Channel 6 was achieved using a complex multi-layer interference filter coating on the focusing lens. Other element in the optical path, especially the detector, have an effect on the overall spectral response. The interference filter is also fairly temperature sensitive. The system verification tests were performed with the filter at room temperature. At orbital operating conditions, the filter temperature will be approximately 200K. This will broaden the bandpass slightly. These results, as well as the measured responses for the visible channels, are shown in Table 3-2.

Table 3-2  
SPECTRAL RESPONSE CHARACTERISTICS, CHANNELS 1-6

<u>CHANNEL</u>	<u>LOWER 50% WAVELENGTH</u>	<u>UPPER 50% WAVELENGTH</u>
1	431.6 nm	453.6 nm
2	510.2 nm	530.8 nm
3	540.6 nm	560.6 nm
4	659.6 nm	678.6 nm
5	698.5 nm	799.0 nm
6 (In Lab)	10.65 μm	12.5 μm
6 (In Space)	10.55 μm	12.45 μm



### 3.4 POLARIZATION SENSITIVITY

Much of the incident radiation from the earth to the instrument is highly polarized. From a radiometric standpoint, it is important that the instrument be insensitive to the state of polarization and measure only the intensity of the radiance. This was accomplished by the use of depolarizing wedges and careful analysis and design of the optics prior to the wedges.

Protected silver coatings, having good reflectance in the blue region and the lowest polarization, are used on the scan mirror, the two telescope mirrors, a folding mirror, and the collimating mirror. The folding mirror is positioned for near compensation of the scan mirror polarization.

Extensive design and analysis went into the depolarization wedges. Measurements showed that when the two wedges that make up the depolarizer are properly adjusted, monochromatic light transmitted through the wedges varies less than 0.5 percent in intensity regardless of its state of polarization.

Measurements were made of the overall instrument's polarization sensitivity in channels 1 through 4 with the scan mirror in three positions. We found it difficult to alter the plane of polarization over  $360^\circ$  and over the entire collecting aperture and still hold the intensity constant to within 1 percent or less. Therefore, the results in Table 3-3, while very acceptable, are probably worse than the actual instrument performance.

Table 3-3  
POLARIZATION IN CHANNELS 1-4 AT THREE TILT ANGLES

<u>CHANNEL</u>	<u>TILT UP <math>10^\circ</math></u>	<u>NADIR</u>	<u>TILT DOWN <math>10^\circ</math></u>
1	2%	1.73%	2.67%
2	1.33%	0.88%	1.04%
3	1.28%	0.76%	0.69%
4	1.05%	1.11%	0.68%



These results indicate that if the scene is polarized 50 percent, the worst case data error would be 1.6 percent.

### 3.5 SCAN TILT

One of the most important features of the CZCS design is its ability to tilt the scan forward or aft of nadir by 350 milliradians or approximately 20° as shown in Figure 3-1. This allows the scan to look away from the sun thus avoiding solar glint, i.e., the specular reflection of the sun from the surface of the water. The relatively high level of the specular reflectance causes channel saturation obliterating the diffuse reflectance which the CZCS is intended to measure.

### 3.6 SIGNAL TO NOISE RATIOS AND NOISE EQUIVALENT TEMPERATURE DIFFERENCE

It is important that the signal to noise ratios (SNR's) for Channels 1 through 5 be high and the Noise Equivalent Temperature Difference (NETD) of Channel 6 be low in order to obtain good radiometric precision. This was achieved on CZCS.

In Channels 1 through 5, the signal out of the detector can be expressed:

$$I_s = N_\lambda A \Omega \epsilon \Delta \lambda S \alpha,$$

where:

$I_s$  = signal current

$N_\lambda$  = radiance incident on the optical aperture

$A$  = area of the optical aperture

$\Omega$  = the small angle field of view

$\epsilon$  = the optical efficiency

$\Delta \lambda$  = the spectral bandpass

$S$  = the detector responsivity

$\alpha$  = an arbitrary degradation factor

Certain of the quantities such as  $N_\lambda$ ,  $\Omega$  and  $\Delta \lambda$  are mission oriented and established. The collecting area of the optics ( $A$ ) was made as large as possible



within the weight and volume values allowed for this instrument. The optical design utilizes reflective elements where possible rather than the lower efficiency transmitting elements such as lenses. The need for lenses and window was minimized and tradeoffs were made for overall optimization of the SNR. Use of a concave grating eliminated the need for an extra mirror or lens. In Channels 1 through 4, the narrow spectral bandpass of a nominal 20 nanometers reduces the signal strength requiring noise minimization techniques to meet the SNR necessary for this mission. This is covered in Section 4.

The NETD for Channel 6 may be expressed:

$$\text{NETD} = (A_d \Delta f_n)^{1/2} (D_{\text{AVE}}^* A_o \Omega \epsilon \alpha \frac{dN}{dT})^{-1},$$

where:

$A_d$  = detector area,

$\Delta f_n$  = equivalent noise bandwidth,

$D_{\text{AVE}}^*$  = the average detector  $D^*$  over the spectral bandpass,

$A_o$  = effective optical collecting area,

$\frac{dN}{dT}$  = the radiance temperature at the specified temperature, and

the other parameters are as previously defined. The main thrust here was to minimize the detector area, optimize optical efficiency and obtain high  $D^*$  detectors. The detector area was minimized by using a fast aplanatic lens immediately in front of the detector. This lens is the prime contributor toward achievement of an optical speed of F/0.64 in Channel 6. Moderately high  $D^*$  detectors were obtained with reasonably high responsiveness. The bipolar transistors used in the preamplifier contributed only a small fraction of the total noise in this channel. A NETD of 0.25K was achieved during thermal vacuum testing of the instrument.

### 3.7 COMMANDABLE GAIN AND THRESHOLD

Commandable gain and thresholding circuits were designed into Channels 1 through 4. Scene radiance varies as a function of solar zenith angle by more



than a factor of 2 for zenith angles from 60° to 10°. In this design, minimum gain was set for the highest expected solar zenith angle of 10°. Gain steps of approximately 1.0, 1.23, 1.5, and 2.15 are implemented by command as shown in Figure 3-4. This figure also illustrates the insertion of an offset which eliminates approximately the lower 70 percent of the signal. A large part of the signal is background. This command allows the elimination of much of the background and enhancement of the remaining 30 percent by an accompanying gain increase of 3.33. The upper 30 percent of the signal is thereby digitized to a full 8 bits. Figure 3-5 illustrates the enhancing effects of this technique.

### 3.8 LINEARITY OF RESPONSE

During reduction of data, computer analysis is minimized if the data can be characterized by a mathematical equation and the error due to that approximation is small. With commandable gain changes such as are found in the CZCS design, it is preferable if the mathematical equation is a straight line function as " $y = mx+b$ ". Repeated measurements made on the CZCS have demonstrated that there is less than a one percent departure from the linear in most channels and less than two percent in all channels. This allows characterization of the output as a function of scene radiance with a slope and intercept value for each channel. The system linearity is a function of detector, amplifier, and analog-to-digital converter linearities. During the design phase, amplifier gains were set conservatively and the A to D converter ladder networks were specified for 10-bit accuracy. In Channels 1 through 5, the detectors are operated in the photoconductive mode by back biasing. This allows linear detector response over several orders of magnitude. In Channel 6, the detector is inherently linear as long as it is not over or under biased. Testing performed at the Honeywell Research Center provided optimum biasing information which was implemented in the design.

### 3.9 MODULATION TRANSFER FUNCTION

The modulation transfer function (MTF) of an instrument is the measure of the ability of that instrument to respond to spatial frequencies inherent in the scene as it scans. The response of the instrument output to a high contrast

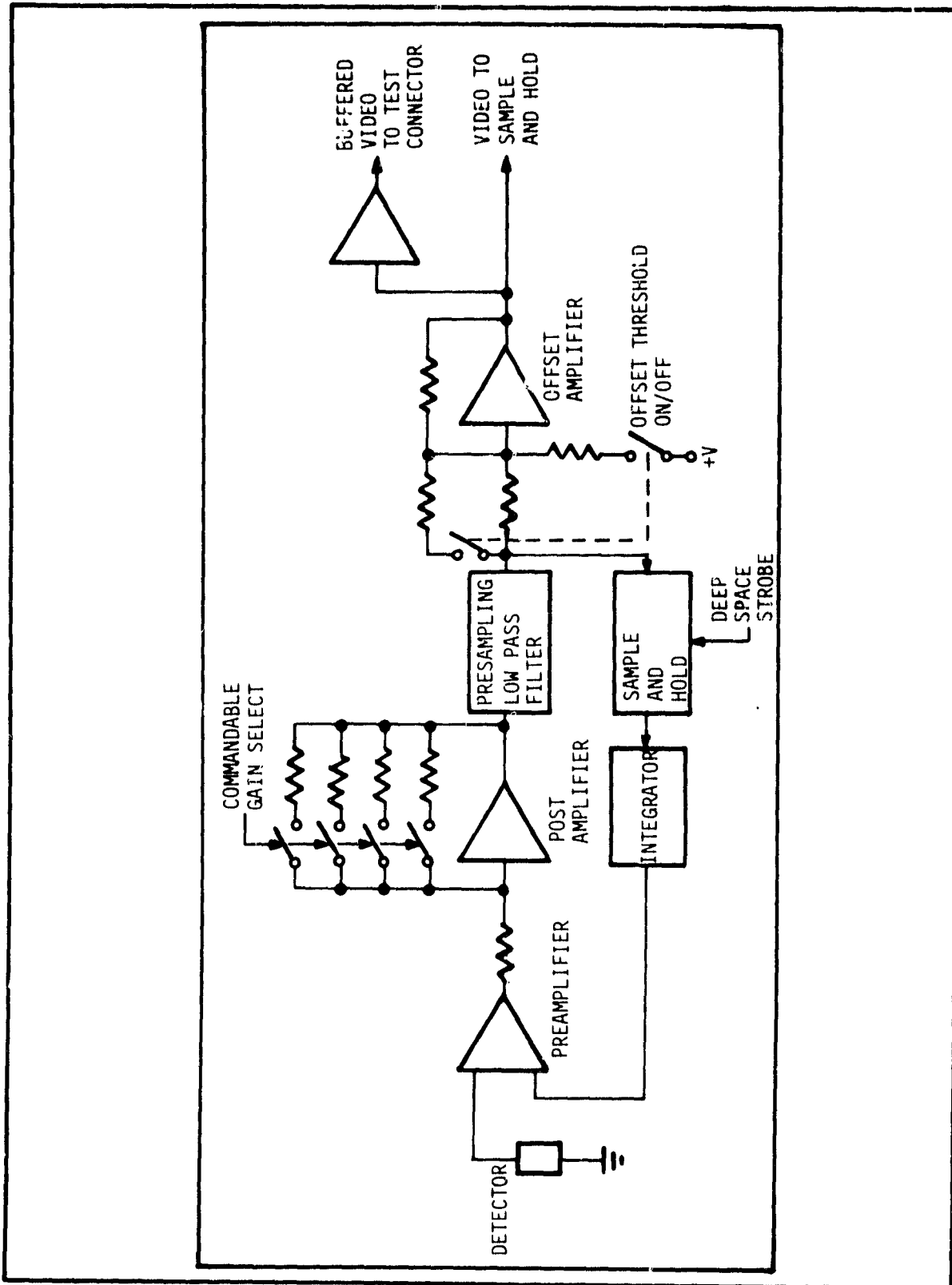


Figure 3-4 Video Channel 1 Through 4 Gain and Threshold

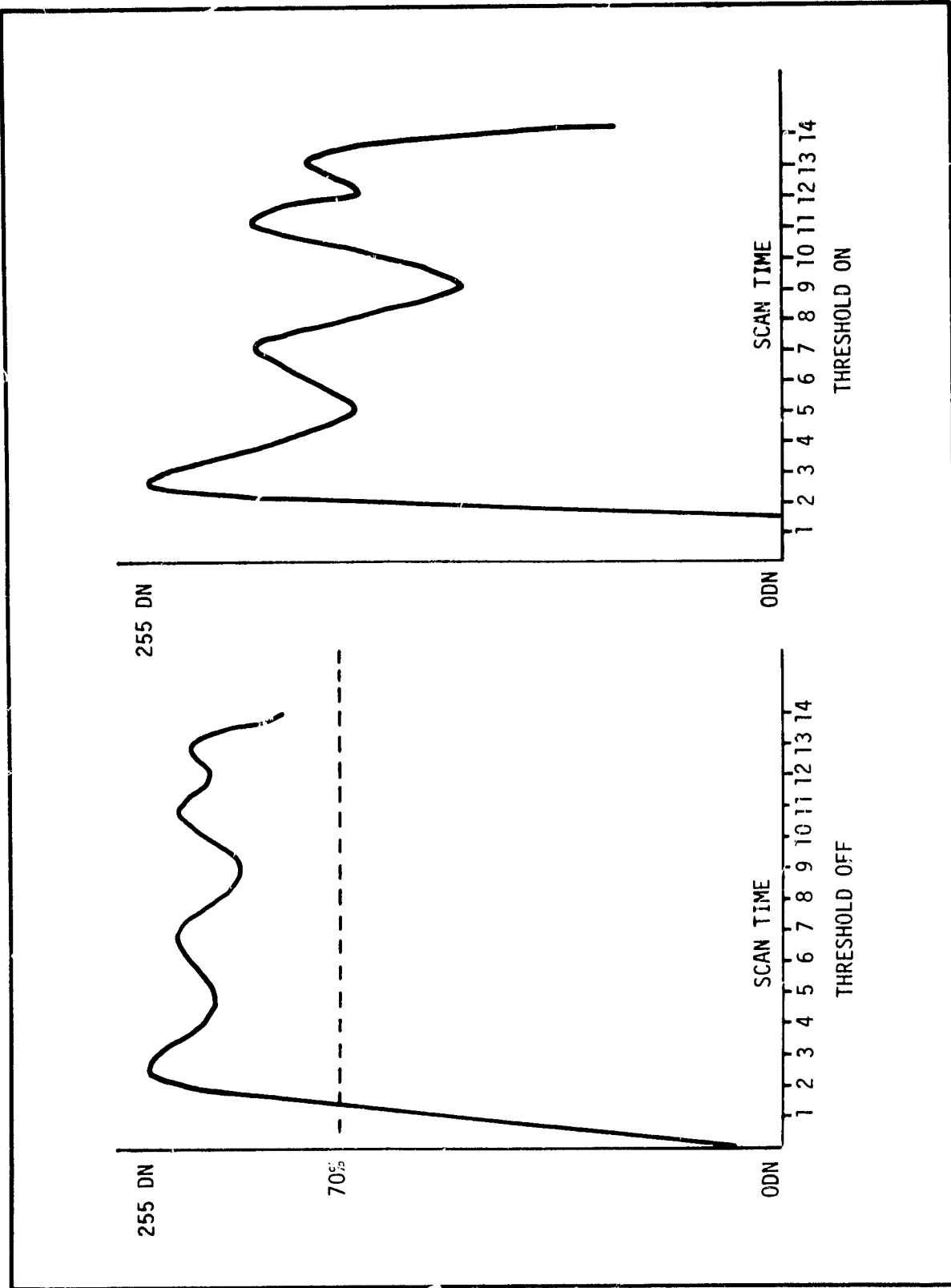


FIGURE 3-5 CHANNEL 1-4 THRESHOLDING EFFECT





scene, i.e., black to white in Channels 1 through 5 and cold to hot in Channel 6, which is modulated at some spatial frequency will drop off at frequencies corresponding to the limiting resolution is:  $(2 \text{ IFOV})^{-1}$ . Since the nominal resolution is 0.865 milliradians, the spatial frequency corresponding to that is 578 cycles per radian. Generally a MTF of 10 percent to 45 percent is desired at the limiting resolution in response to a bar pattern which generates a square wave at the limiting frequency. While MTF is, to be perfectly correct, a sinusoidal function, the use of the bar pattern is an expedient due to the relative difficulty involved in generating a sinusoidal pattern.

There are four contributors to the CZCS MTF. They are:

1. Spatial - As the instrument scans the subsatellite or nadir direction, the IFOV is a square image. Its Fourier transform in the scan direction is a  $\frac{\text{SIN } X}{X}$  function which converts from an image to the spatial frequency domain. At a frequency corresponding to the limiting resolution, the sinusoidal MTF is  $\frac{2}{\pi} \text{SIN } \frac{\pi}{2}$  or 0.637.
2. Optical - The optical MTF is a function of diffraction and optical aberrations. If care is taken in the design and fabrication of the optics, images can be made sharp and crisp with resulting good MTF. As aberrations increase, the images get fuzzy and less distinct and the MTF suffers. Diffraction effects increase with wavelength and the optical MTF of Channel 6 is not as good as the first five channels. The calculated MTF in Channels 1 through 5 is 100 percent while Channel 6 is 94 percent.
3. Electrical Presampling Bandwidth - Each channel is filtered prior to sampling and digitization to limit the noise. Considerations in selecting this bandwidth are noise, MTF, and the sampling rate. In the CZCS this bandwidth is set to the electrical frequency corresponding to the limiting resolution spatial frequency. At that frequency the electrical MTF is 0.707.
4. Sampling Rate - The sampling rate is fixed at 72.73 kilohertz which corresponds to the previously discussed 13.75  $\mu\text{sec}$  interval. Conversion of this step function from a time to a frequency domain by Fourier transform is also a  $\frac{\text{SIN } X}{X}$  function. At 578 cycles per radian, its MTF is 0.756. The sampling frequency is 2.5 times the electrical bandwidth which minimizes aliasing errors.



To convert from sinusoidal to squarewave MTF, the sinusoidal components associated with the primary frequency of interest and its odd harmonics are summed as follows:

$$MTF_{sw}(v) = \frac{4}{\pi} [MTF_{si}(v) - \frac{1}{3} MTF_{si}(3v) + \frac{1}{5} MTF_{si}(5v) - \dots]$$

where:

sw denotes squarewave, si denotes sinusoidal and v denotes spatial frequency. Squarewave measurements performed are summarized by Table 3-4.

Table 3-4  
CZCS CHANNEL MTF'S AT TWO SPATIAL FREQUENCIES

<u>CHANNEL</u>	<u>MTF at 289 cycles/rad</u>	<u>MTF at 578 cycles/rad</u>
1	0.91	0.383
2	0.886	0.378
3	0.974	0.464
4	0.911	0.444
5	0.918	0.402
6	0.900	0.368

### 3.10 CZCS/SPACECRAFT DATA HANDLING INTERFACE

While the average data rate from the CZCS is about 800 kilobits per second (see Section 3-2), the maximum data rate is slightly less than 3.5 megabits per second. The ZIP or CZCS Information Processor provides a buffering and formatting function for interfacing with the spacecraft tape recorders and downlink.

Figure 3-2 (Section 3.2) shows the organization of the data window which determines which data is to be digitized (undigitized data comes to the ZIP as digital "ones"). The relationship of the data window to scan mirror positions is illustrated by Figure 3-3. The CZCS sends not only science and housekeeping



data to the ZIP in an eight bit parallel format but also the data window and a line sync pulse. The latter indicates the start of a new scan line of information from CZCS. The ZIP provides the CZCS with a 1.6 megahertz clock and a sample line with a pulse period of 13.75 microseconds. Within a 123.75 millisecond scan line, the sample line provides 9,000 sample periods, i.e. 9,000 possible analog-to-digital conversions for each CZCS channel. The sample line from ZIP is reset by each line sync pulse so that data sampling is synchronized with the line sync each line. Table 3-5 illustrates the flow of data to the ZIP. Notice that the "x's" indicate non-meaningful data and occur at points outside the data window. Since the ZIP is also provided the data window, it will recognize only good data from the CZCS. The data is organized by channel with all data generated by that channel except for samples 8096-8099. The housekeeping data function is identical in channel 1 with the corresponding data in channel 2. The temperature monitor for the blackbody target is also found in channel 6 during these samples.

The ZIP then organizes the CZCS data along with the sync words, frame identification words and time code into a 925 word by 15 minor frame structure. This is shown by Figure 3-6. The sync, frame identification, time code, and fill words are provided by the ZIP. The earth scan data from the CZCS is organized into 384 words x 15 minor frames and 432 words x 14 minor frames. The remaining 432 words in the fifteenth minor frame included 24 words of active calibration, i.e., channel responses to the internal, inflight sources; 384 words of voltage calibration including four samples each of 16 steps from each channel; and 24 words of housekeeping data, 12 of which are fill words. That this interface has worked out so well at the spacecraft level is due, in large part, to the numerous interface meetings attended by GSFC, BASD, General Dynamics, and General Electric personnel. The same data organization used by the ZIP was also used in the CZCS Bench Check Unit which allowed several problem areas to be identified and corrected prior to bench integration tests.



TABLE 3-5 -- CZCS SCIENCE DATA FORMAT (ZIP DATA)

NOTE: The sequence of data shown in this table represents a single scan line, as generated by a single revolution of the scan mirror. The table shows that 9000 sample lines occur between each consecutive pair of scan line-sync signals. The X's in the table are not meaningful data, being inserted as 1's into the data train for spacing and timing purposes. The number in the "Sample" column represents the number of sample lines from the previous scan line sync (excluding the first such sample line).

CHANNEL NUMBER						SAMPLE	EXPLANATORY REMARKS
1	2	3	4	5	6		
X	X	X	X	X	X	1	<p>Blackbody calibration of Channel 6 occurs during each and every scan. Channels 1-5 calibration occurs only in those scans when subcom ID is 15 or 31. For other subcom ID's Channels 1-5 are all X's.</p> <p>DC Restorer interval is between 7798 and 8024.</p> <p>(1) There are 32 channels of subcom data. One channel is identified and sampled (four times) in each scan.</p> <p>(2) Blackbody temperature is sampled four times in each scan. This particular monitor is conditioned separate from the BB-Temp monitor read through the VIP analog channel and through the subcom.</p>
X	X	X	X	X	X	↓	
X	X	X	X	X	X	113	
Earth-Scan Radiance Data						114	
						↓	
						2081	
X	X	X	X	X	X	2082	
X	X	X	X	X	X	↓	
X	X	X	X	X	X	5595	
Active Radiance Calibration Visible-Light Channels (Lamp-Shutter)					IR (BB)	5596	
						↓	
						5599	
X	X	X	X	X	X	5600	
X	X	X	X	X	X	↓	
X	X	X	X	X	X	8027	
Voltage Calibration (Voltage Step 1)						8028	
						↓	
						8031	
Voltage Calibration (Voltage Step 2)						8032	
						↓	
						8035	
Voltage Calibration (Voltage Steps 3 through 15)						8036	
						↓	
						8087	
Voltage Calibration (Voltage Step 16)						8088	
						↓	
						8091	
X	X	X	X	X	X	8092	
X	X	X	X	X	X	↓	
X	X	X	X	X	X	8095	
Subcom I.D. (1)	Hskpg. Data (1)	X	X	X	Blackbody Temp. (2)	8096	
		X	X	X		8097	
		X	X	X		8098	
		X	X	X		8099	
X	X	X	X	X	X	8100	
X	X	X	X	X	X	↓	
X	X	X	X	X	X	9000	

← Line Sync from Scanner

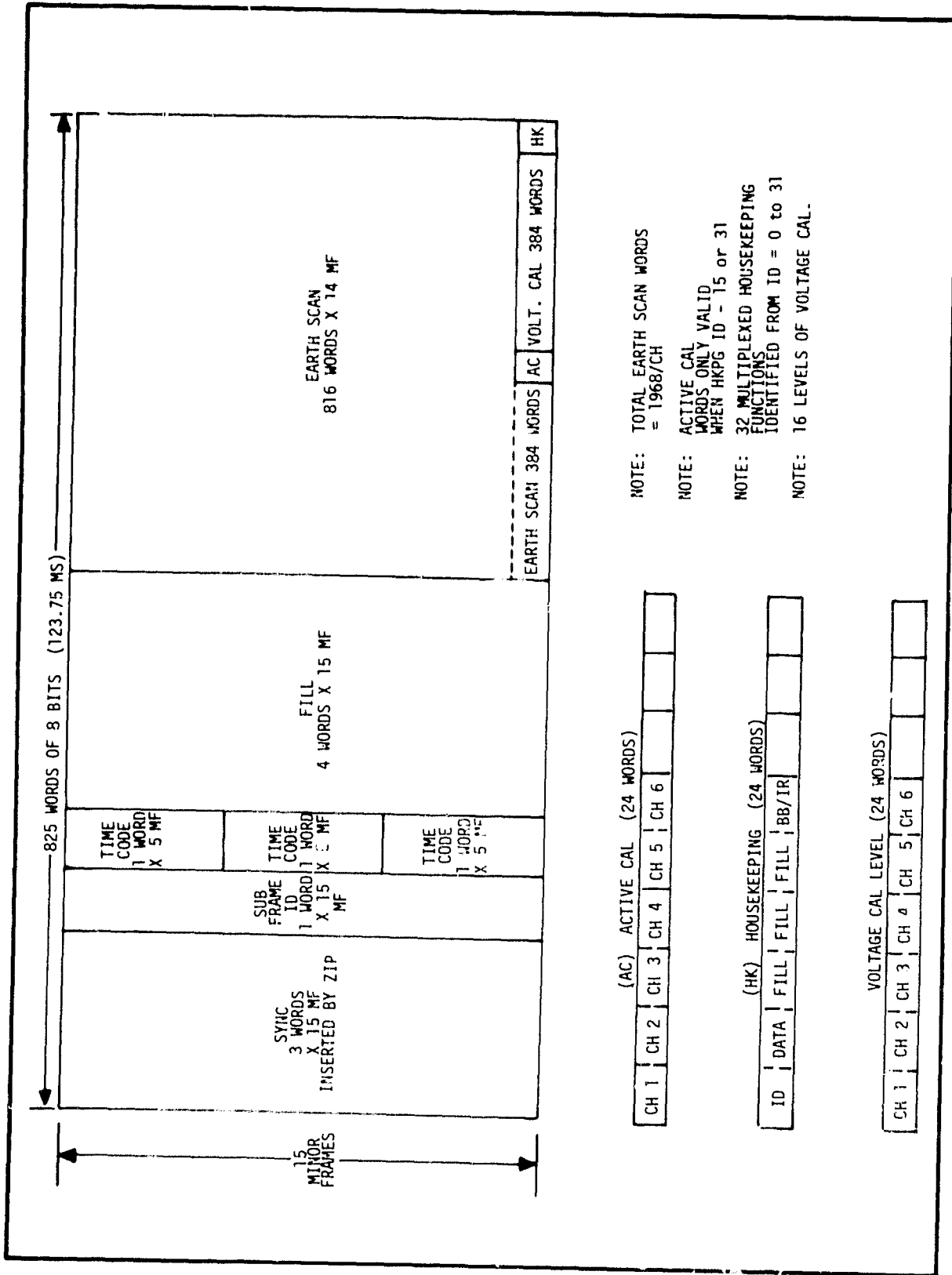


Figure 3-6 ORGANIZATION OF CZCS DATA BY ZIP



## Section 4 DESCRIPTION OF CZCS SUBSYSTEMS

The CZCS instrument is designed for modularized assemblies for accessibility and maintenance. The six major CZCS subsystems are the structure, optical, scanner, scanner electronics, main electronics, and analog electronics. Each subsystem is a physical entity and can be tested as a separate entity. The block diagram provided in Figure 4-1 shows, in capsule form, the functions of each subsystem. The major elements of the CZCS are shown in Figure 2-2 (Section 2) to better illustrate how the subsystems fit together. In the following sections, the elements and functions of the major subsystems are described (for additional information see the CZCS Operation and Maintenance Manual).

### 4.1 STRUCTURE SUBSYSTEM

The CZCS structure is the simplest of the subsystems and is an optical bench upon which the other subsystems are mounted. It includes, beside the mechanical structure shown in Figure 4-2, the blackbody target and various temperature sensors. Intersubsystem cabling is also mounted to the structure. The structure is assembled of a number of separately fabricated aluminum parts and electron beam welded to the unibody construction shown by Figure 4-2. The structure has been designed for minimal amplification of vibrational inputs at the mounting interface to the subsystem interfaces.

### 4.2 OPTICAL SUBSYSTEM

The optical subsystem has been designed for separate assembly, alignment, and test. It includes a mechanical structure to which the other elements are attached known as the telescope plate, a telescope assembly, a spectrometer assembly, a radiative cooler assembly, a cooler door assembly, and optical elements for Channel 6.

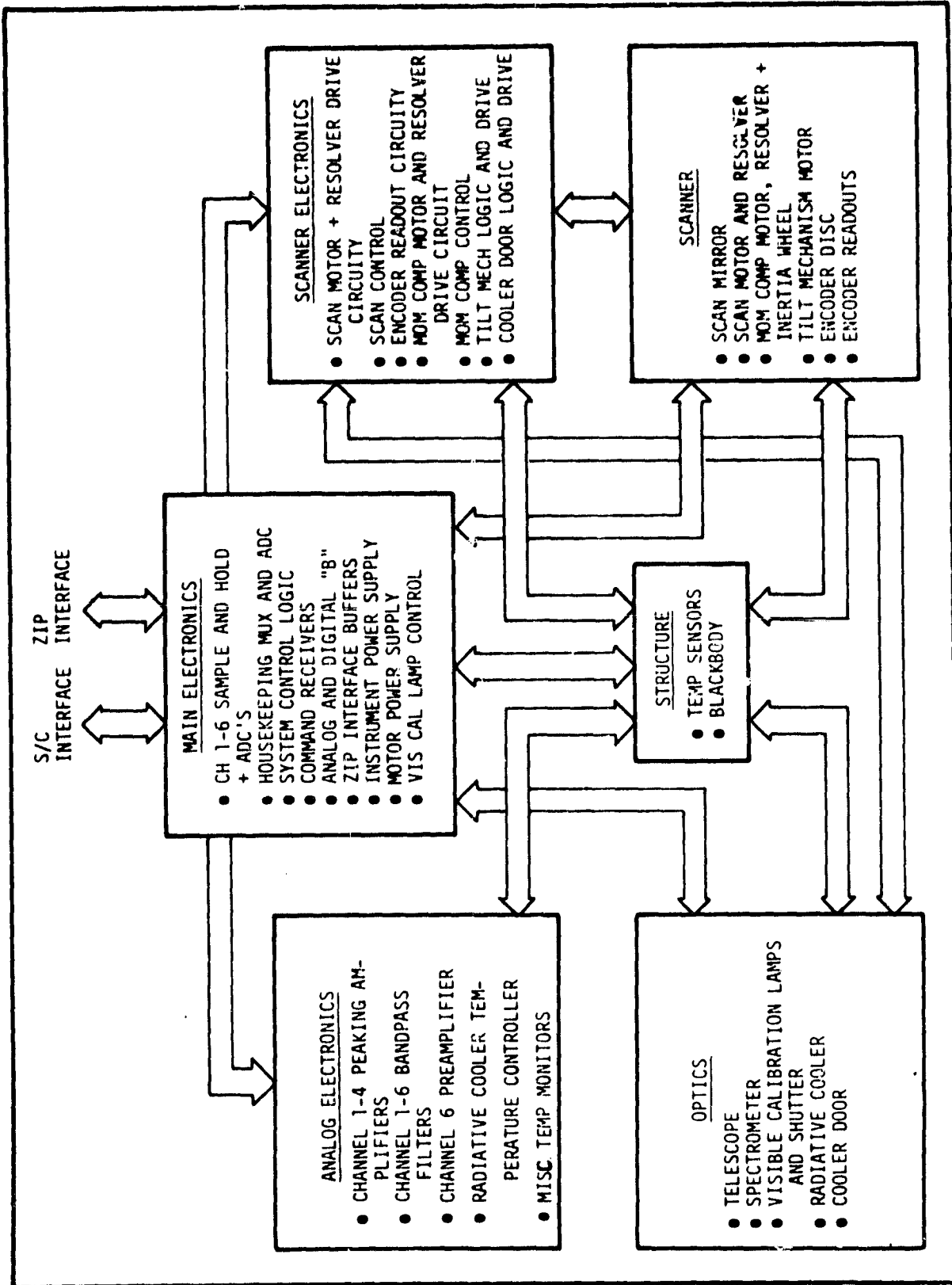
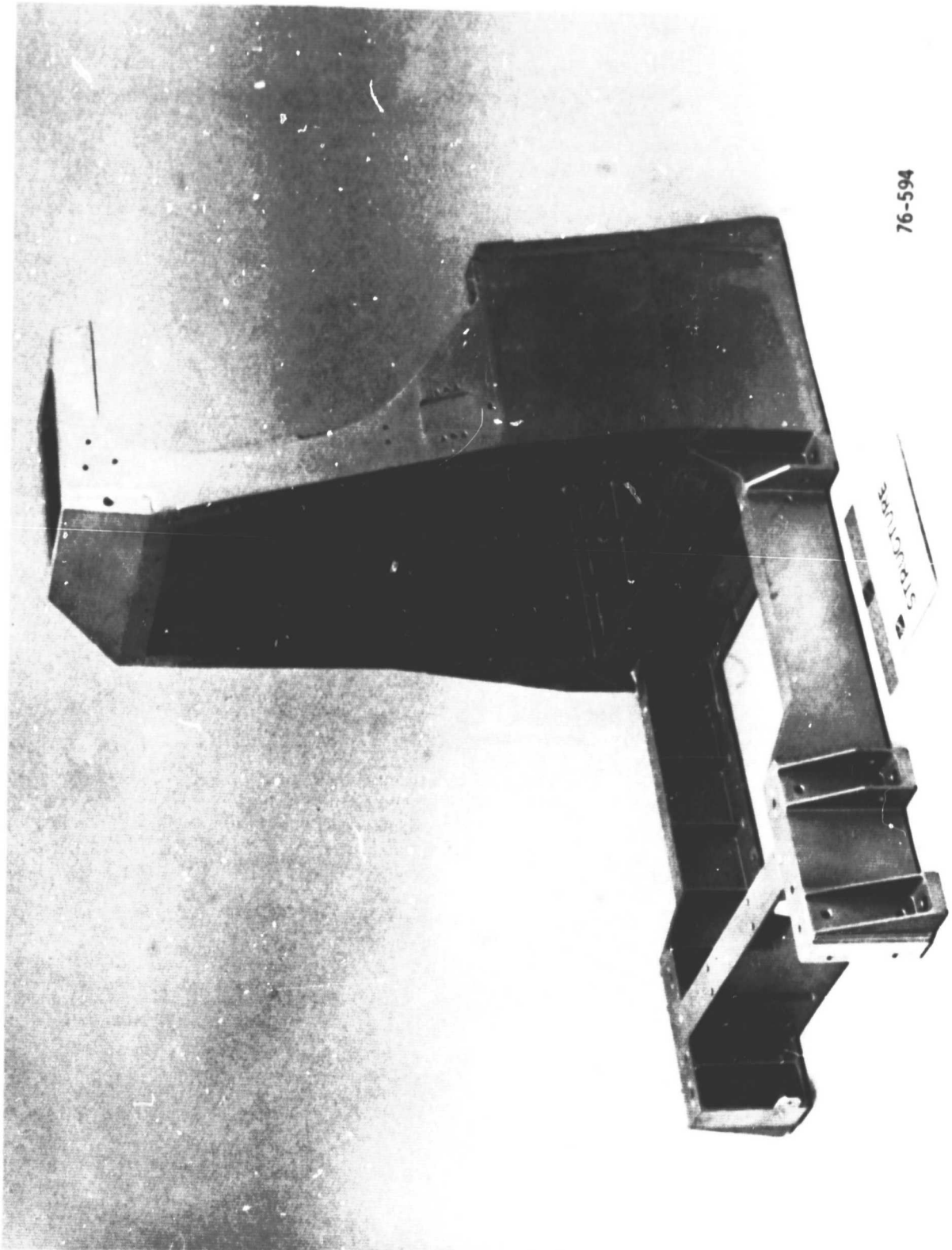


FIGURE 4-1 CZCS SUBSYSTEM INTERRELATION BLOCK DIAGRAM



76-594

Figure 4-2 CZCS Main Structure





#### 4.2.1 Telescope Assembly

The telescope assembly includes the primary and secondary mirrors of the classical cassegrain system; a beamsplitter to separate infrared radiance for Channel 6 from shortwave radiance for the other channels; a baffle to minimize scattered and out-of-field radiance effects; and a folding mirror and field lens for Channel 6. These components include those shown in Figure 4-3 up to and including the field lens, L-6. They are contained in and attached to a tubular Invar structure for minimal temperature distortion and misalignment. Also included in the telescope assembly are the field stop and folding mirror M-6 located at the central hole of the primary mirror.

#### 4.2.2 In-Flight Calibration

In-flight calibration targets have been included in the CZCS design for the visible channels, i.e. Channels 1-5 and the IR Channel, i.e., Channel 6. The latter is a honeycomb blackbody located in the structure for viewing by the entire optical system at the scan angle of  $180^\circ$  from nadir. No attempt is made to control the temperature of this target; it varies with the instrument. Being located between four of the mounting feet and nearly at the spacecraft interface mounting plane, its temperature is not expected to vary widely (see Figure 2-2). The temperature of the blackbody target is monitored by a thermistor located at its center. Readout accuracy by the VIP telemetry system is approximately  $0.11^\circ\text{C}$ .

The visible channel calibration system is located in the spectrometer for calibration of the spectrometer optics and the detectors for Channels 1-5. Light from this source is introduced to the spectrometer through a hole in the collimating mirror, M-7. It provides a checkout of the depolarizer, mirrors M-8 and M-9, the grating, the field lenses and the detectors. A schematic of the visible calibration optics is shown in Figure 4-4. Either of two redundant lamps may be used with the beamsplitter providing a transmissive path for one lamp and a reflective path for the other lamp. Since there is a difference between the reflection and transmission of the beamsplitter, response to the two lamps is unequal. The lamps are operated at a temperature of approximately

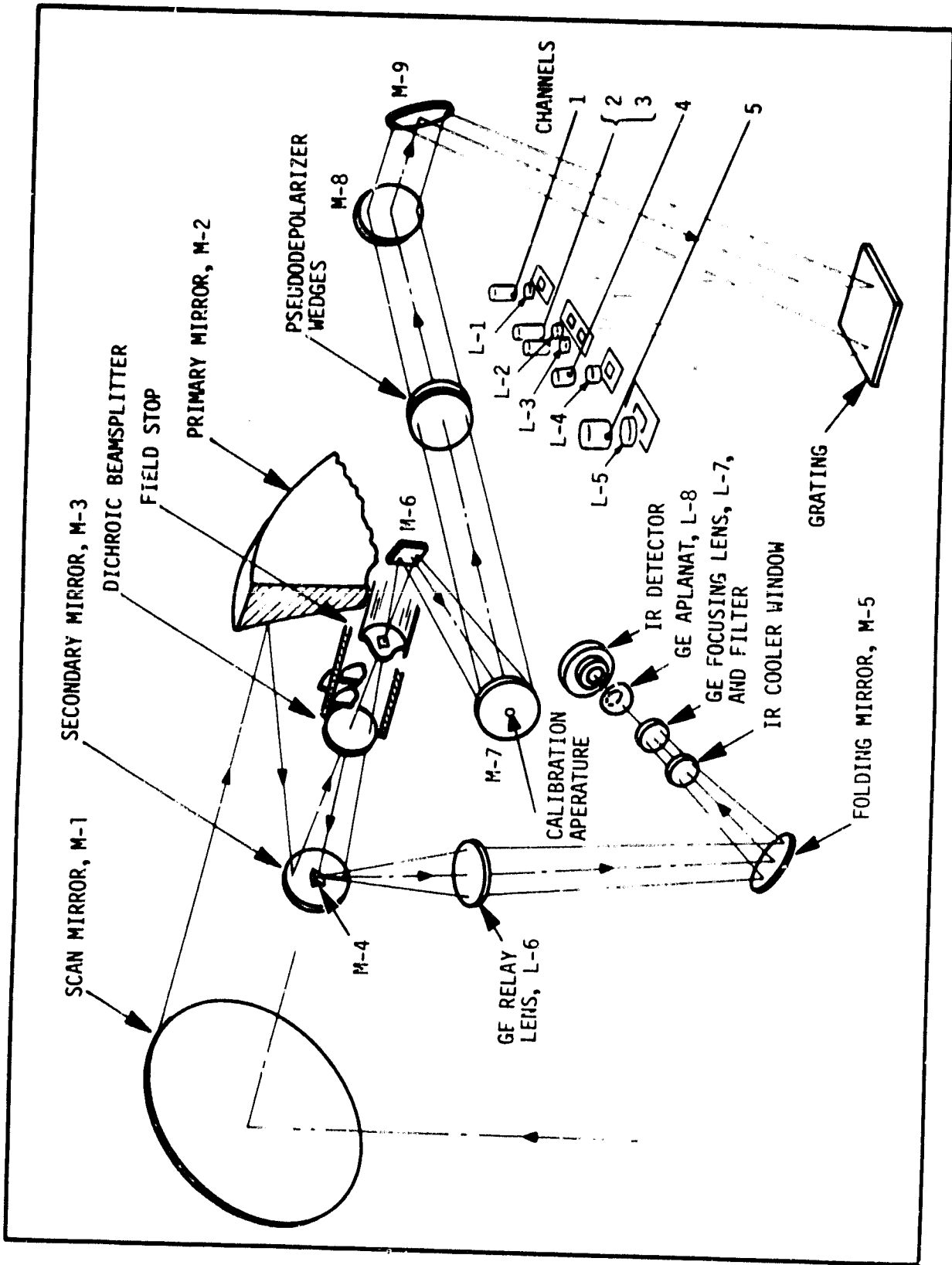


Figure 4-3 OPTICAL ARRANGEMENT

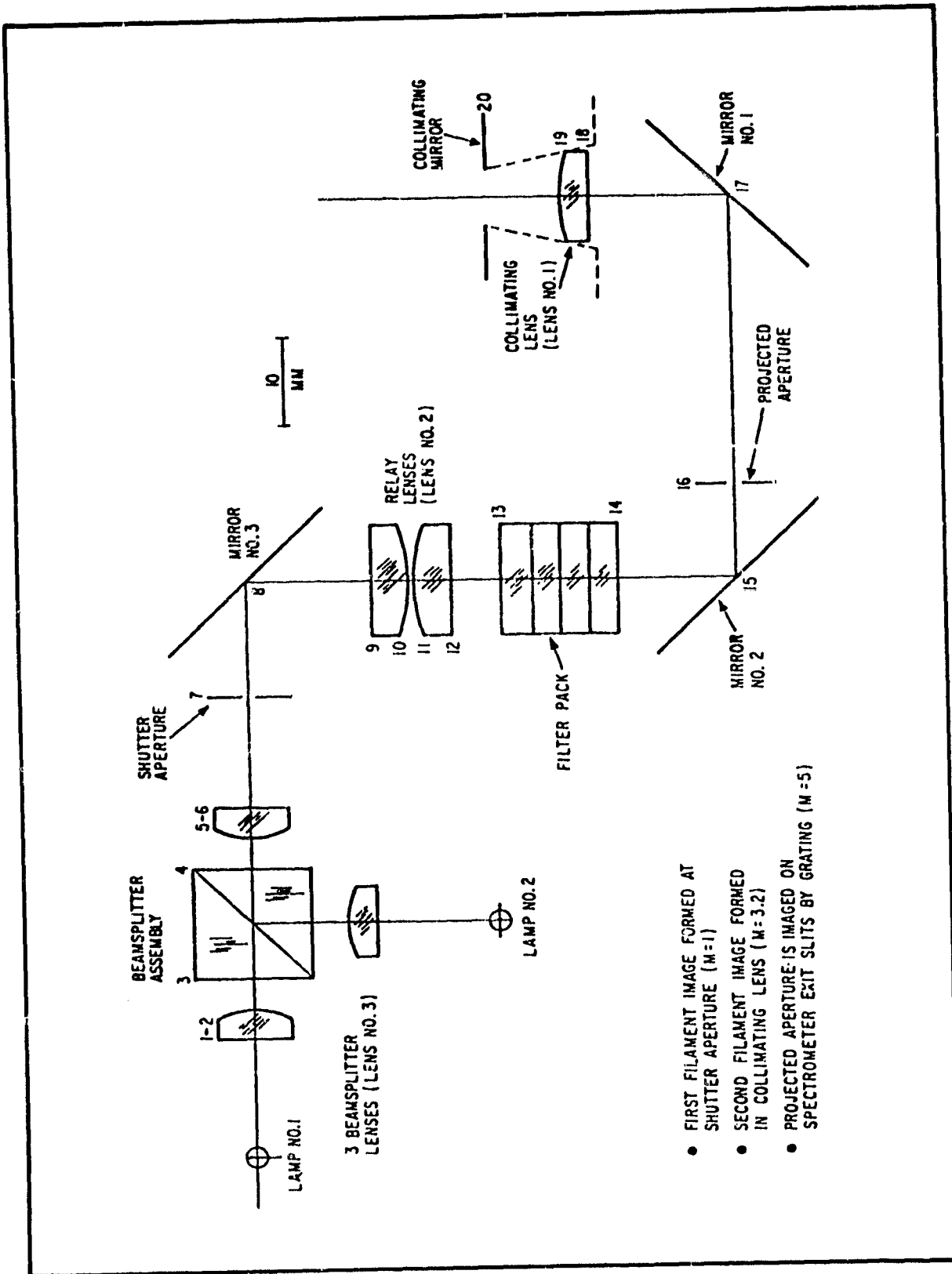


Figure 4-4 VISIBLE CALIBRATION OPTICS



2000K. To peak the response more toward the blue end of the spectrum, i.e., better simulate a solar spectra, a group of four filter glasses were selected for reasonably good response in all channels under various gain settings. The output is collimated by lens No. 1 located in the collimating mirror of the spectrometer. The lamp current is selected for each of the lamps for the proper temperature and channel response. Separate constant current sources are used to power each lamp. Selection of either of the two lamps is accomplished by commands. The shutter automatically opens and closes during the backscan. Data are taken after the shutter blade settles and prior to start of closure.

#### 4.2.3 Spectrometer Assembly

The spectrometer assembly attaches to the telescope plate with the housing pinned for repetition of optical alignment with the telescope. The entire outboard side of the housing is a cover which is removable for assembly, adjustment and troubleshooting. Attached to the cover is a removable contamination witness mirror which is not flown. A partially disassembled spectrometer is shown in Figure 4-5.

The spectral responses of Channels 1 through 5 are set by the grating spectrometer which includes, as shown in Figure 4-3, mirrors M-7, M-8, and M-9, the depolarized wedges, the grating, lenses L-1 through L-5, the exit slits, and the detectors. While mirror M-6 and the field stop are a part of the telescope assembly, they are integral parts of the functioning spectrometer. The spectrometer is a Wadsworth arrangement with a spherical mirror (M-7) on the input side and a 600 line per millimeter concave grating on the output side. The telescope forms a real image at the field stop which is relayed and reimaged at the exit slits. The field stop serves as the entrance slit to the spectrometer. The diverging beam (F/4) through the field stop is folded by M-6 and collimated by M-7. After the collimated beam passes through the depolarized wedges, it is directed by mirrors M-8 and M-9 to the grating. The concave grating is an aluminized replication blazed at approximately 450 nm. Being concave, it converges the beam, but spectrally disperses it to the exit slits. The field lenses (L-1 through L-5) permit the use of smaller detectors and, in Channels 4 and 5, are made of Schott SF1G7 to block second order spectra. The exit



76-506

Figure 4-5 Spectrometer Assembly

ORIGINAL PAGE IS  
OF BEST QUALITY



slits are adjustable and were adjusted for optimum performance.

#### 4.2.4 Channel 6 Optical Elements

The Channel 6 optics are shown in Figure 4-6. All of these except mirror M-5 are located in either the telescope or radiative cooler assemblies. Mirror M-5 provides an interface between these two assemblies. It has multidimensional adjustments for coalignment of the Channel 6 image with the field stop image for Channels 1 through 5.

In Channel 6 the spectral response is mainly established by the interference filter/focusing lens L-7. The detector's spectral response has a very noticeable effect on the overall response while the field lens (L-6) the cooler window and the aplanatic lens (L-8) have minor effects. The latter are all made of germanium and have broadband antireflection coatings. Mirrors M-1, M-2, and M-3 have protected silver coatings while M-4 and M-5 are gold coated. The dichroic beamsplitter has a thin gold coating. The responses of all of these reflective elements are flat from 10.5 to 12.5  $\mu\text{m}$  and have a negligible effect on the Channel 6 spectral response. Measured 50 percent wavelengths are 10.65  $\mu\text{m}$  to 12.5  $\mu\text{m}$ . These measurements are made on the bench with the filter at room temperature. At orbital operating conditions, the filter temperature will be approximately 200K. This will broaden the bandpass slightly causing the 50 percent wavelengths to become 10.55  $\mu\text{m}$  and 12.45  $\mu\text{m}$ .

#### 4.2.5 Radiative Cooler Assembly

The radiative cooler, which also attaches to the telescope plate, is an assembly procured from A.D. Little, Inc. The radiative cooler is shown mounted to the CZCS in Figures 2-1 and 2-2. It is designed to cool the channel six detector mounted to the inner stage to less than 120K by radiative coupling to space. Its conical design restricts its field of view to  $101^\circ$  to minimize earth and spacecraft radiative coupling. Vacuum chamber tests verified the cooling capabilities of the radiative cooler. Also included in the cooler are optical elements L-7 and L-8, the cooler window and the IR detector. The IR detector and the aplanatic lens (L-8) with a housing form a separate assembly.

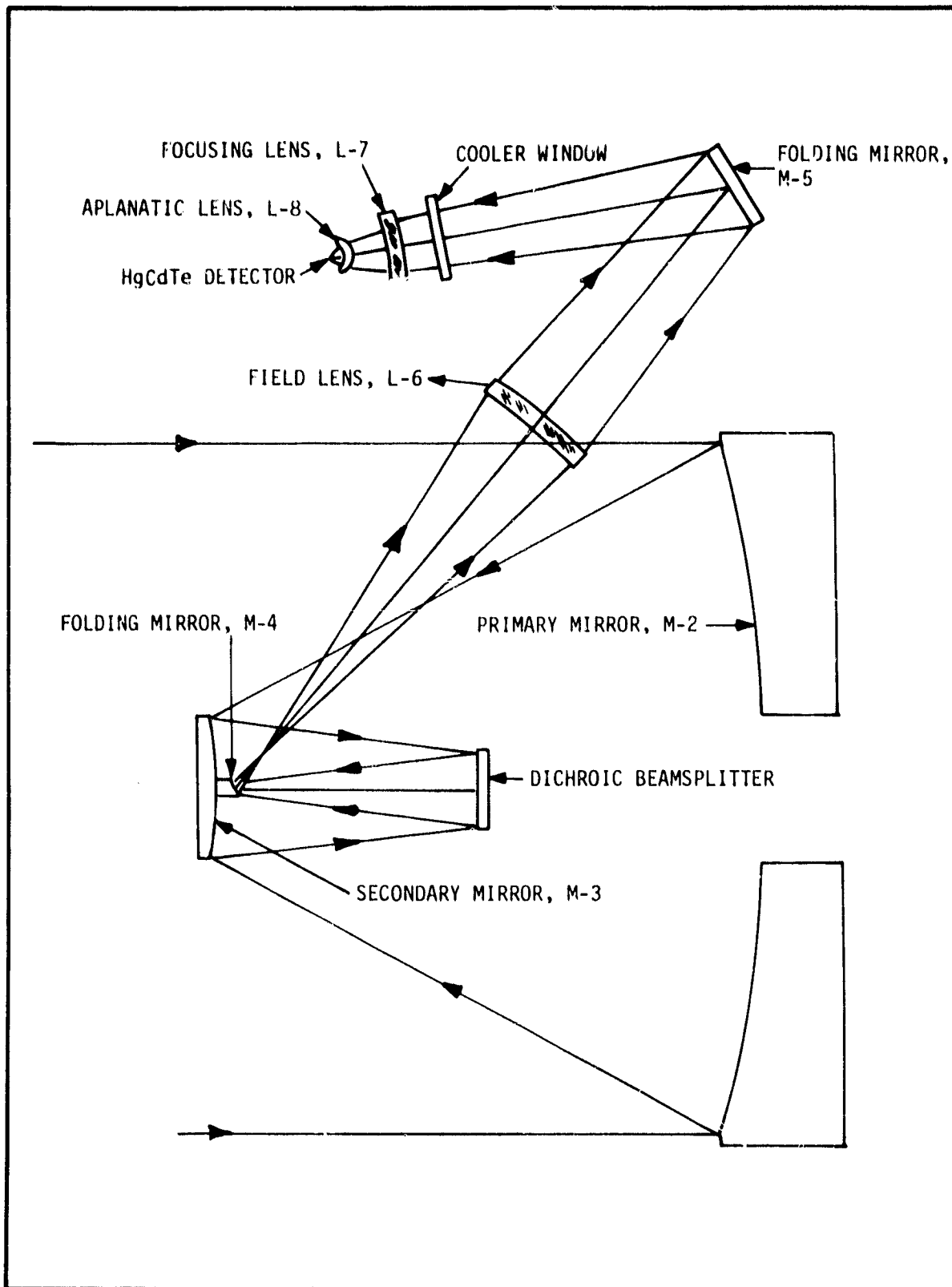


FIGURE 4-6 CHANNEL 6 OPTICS



#### 4.2.6 Cooler Door Assembly

The door for the radiative cooler is opened and closed on command by a stepper motor/gearhead assembly. After launch the first command to open the door also releases a latch provided to hold the door closed during launch. A fail-safe backup door opening mechanism is also provided. By command, heat is applied to a composition shear pin which shears when heated and softened to allow the spring loaded door to open. The door is opened to permit detector cooldown and when opened functions as an earth shield for the cooler. Closing of the door allows warmup of the cooler and elimination of any buildup of contaminating elements.

#### 4.3 SCANNER SUBSYSTEM

The scanner subsystem is shown in Figure 4-7. It provides the scan mirror drive and tilt, and momentum compensation for the scan mirror drive. Included in the scanner subsystems are:

- The scan mirror, scan mirror shaft, and dynamic balance counter weights.
- The scan drive assembly including a brushless d.c. torque motor, a resolver for motor commutation, an optical encoder for velocity and once around (line sync) information, and the light emitting diodes, and photo-transistors for pickup.
- The momentum compensation including a brushless d.c. torque motor and resolver and an inertia wheel.
- The tilt mechanism including a stepper motor and gearhead, screw drive, potentiometer for position readout and a launch caging mechanism.
- The motor housing, bearings and the trunnion which attaches to the structure.

The scan mirror is weight-relieved beryllium, plated with electroless nickel and overcoated with protected silver. It is driven in phase lock at 8.08 Hz or 485 RPM. The momentum due to the scan mirror and its drive is compensated by the counter-rotating momentum compensation to within a measured residual value of 5.2 gm-cm-sec or 0.045 percent of the scanner momentum.



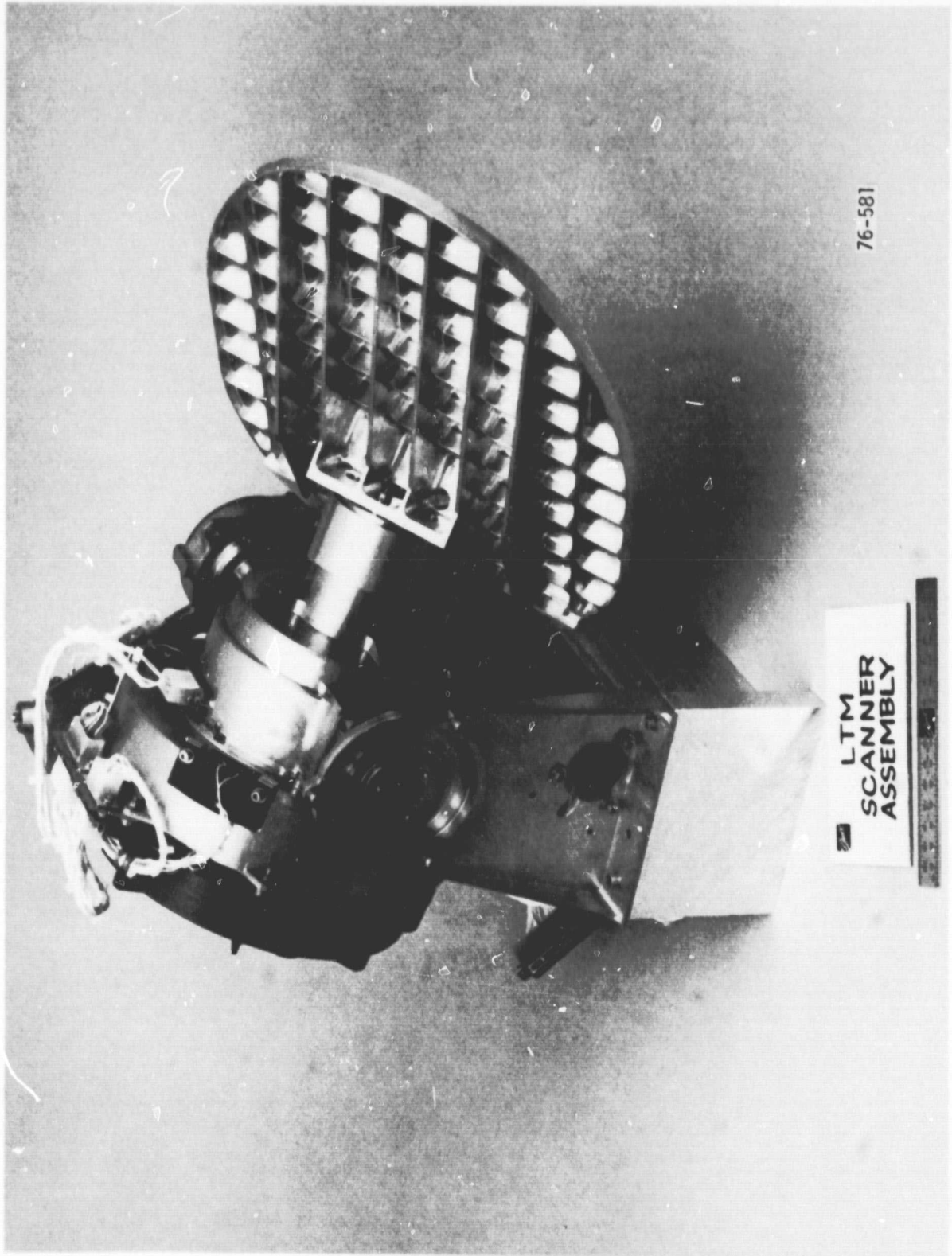


Figure 4-7 Scanner Subsystem

ORIGINAL PAGE IS  
OF POOR QUALITY



The 3 sigma value of 4,800 contiguous line to the line period differences for the CZCS scan drive under vacuum conditions was 1.77 microseconds. The average period was 123.74953 milliseconds which means that 99.7 percent of the line to line period differences (or jitter) were less than 0.00143 percent of the scan period. The scan velocity therefore is constant to approximately 1 part in 70,000. The average period is within 0.00038 percent of the design value of 123.750 milliseconds.

The CZCS design to implement the tilt is illustrated by Figure 4-8. A 90° stepper motor is geared down to drive a leadscrew. The leadscrew attaches to the tilt flexure translating the linear motion of the leadscrew to a rotation of the scan drive assembly about the trunnion axis. With the gearhead and leadscrew the system is overdamped and there is no discernable settling time after completion of the stepping sequence. The drive electronics are designed to rotate the mechanism in 1° increments which tilts the scan IFOV 2° or 35 milliradians. At the drive rate of 40 PPS it takes 9.9 seconds and 396 motor steps to complete one 2° scan tilt increment. The design allows for 21 discrete positions; 10 positions forward of nadir, 10 positions aft of nadir and nadir. A step up or down command will start the tilt in the appropriate direction and a stop command given within the 9.9 second interval will stop the tilt after that 2° increment is complete. If two steps are desired, the stop command is given after the time interval for the first increment and prior to the time required to complete the second increment (19.8 seconds). The exact tilt position is readout via the potentiometer which is also used to control an automatic turnoff if 10 increments are exceeded in either direction from nadir. An obvious feature of the design shown by Figure 4-6 is that full momentum compensation is achieved at any tilt angle as the momentum compensator is attached to the scanner. Measurements were made of the individual steps during system test. The results are provided in Table 4-1.

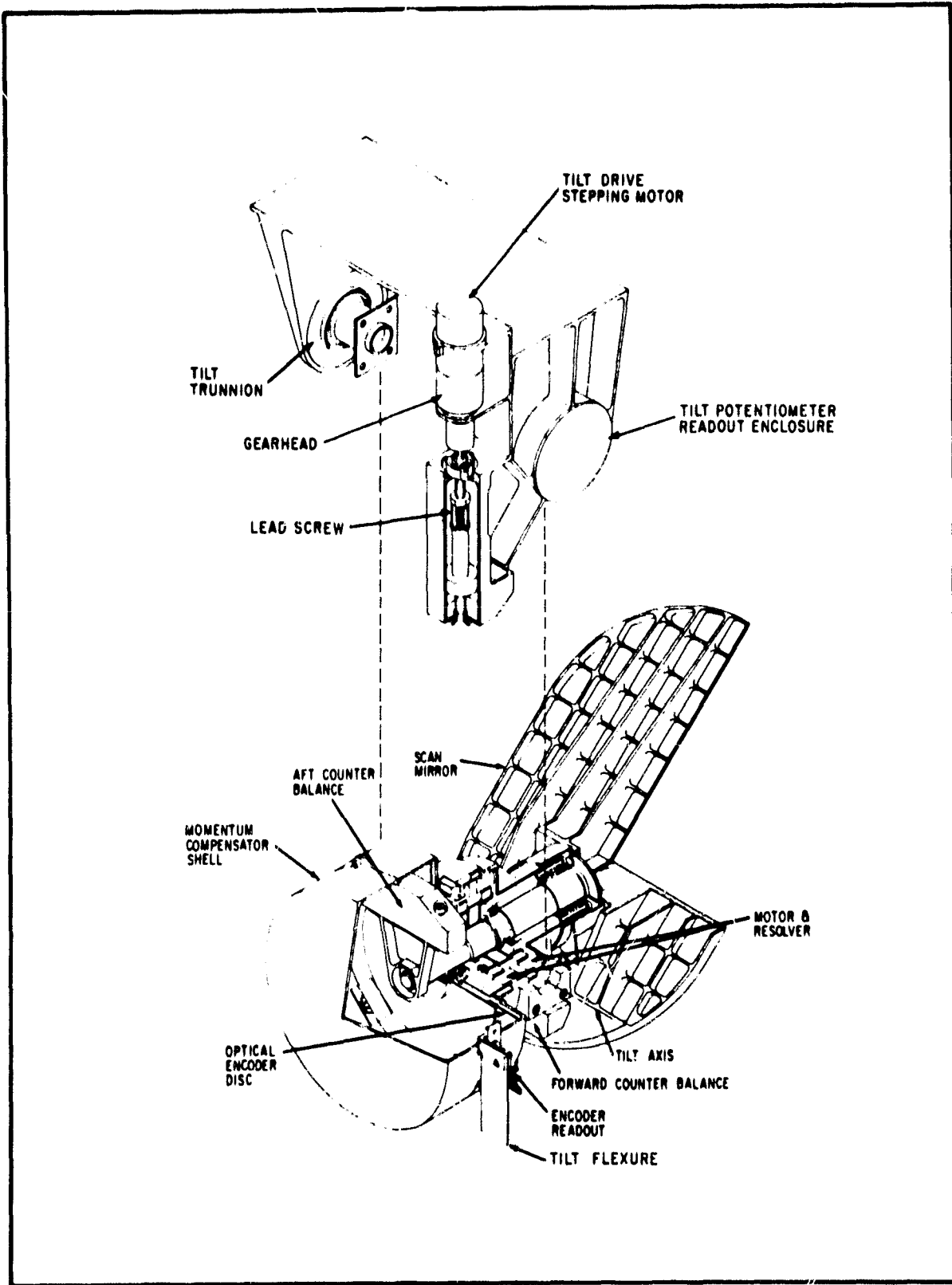


FIGURE 4-8 SCAN TILT IMPLEMENTATION



Table 4-1  
SCAN TILT MEASUREMENTS

<u>Steps From Nadir</u>	<u>Tilt Up (Forward)</u> (milliradians)	<u>Tilt Down (AFT)</u> (milliradians)
1	34.7	34.7
2	69.4	69.4
3	104.2	104.2
4	139.1	139.0
5	174.1	173.7
6	209.0	208.5
7	244.0	243.3
8	279.1	278.2
9	314.4	313.1
10	349.2	347.6

To protect the tilt mechanism in the launch environment, it is locked into position by the launch caging mechanism. In the post launch phase, the caging mechanism is released by the firing of redundant pyrotechnic bellows motors by ground command. This allows the scanner to be tilted freely about the trunnion in normal operation. After assembly and dynamic balancing of both the scan drive and momentum compensator, the scanner subsystem is mated with the Scan Electronics Subsystems for further adjustment and test.

#### 4.4 SCAN ELECTRONICS SUBSYSTEM

The primary function of the Scan Electronics Subsystem is the provision of electrical drives for the scanner, momentum compensator, scan tilt, cooler door and calibration shutter motors. All of the circuitry for ramp up and ramp down of the scanner and momentum compensator, scanner phase lock loop, resolver electronics and power amplifiers is contained in this subsystem. Included also are the logic and drive for the tilt and cooler door mechanisms. Figure 4-9 shows the scan electronics box which houses the eight circuit boards. The Scan Electronics Subsystem is tested prior to integration with the Scanner Subsystem.

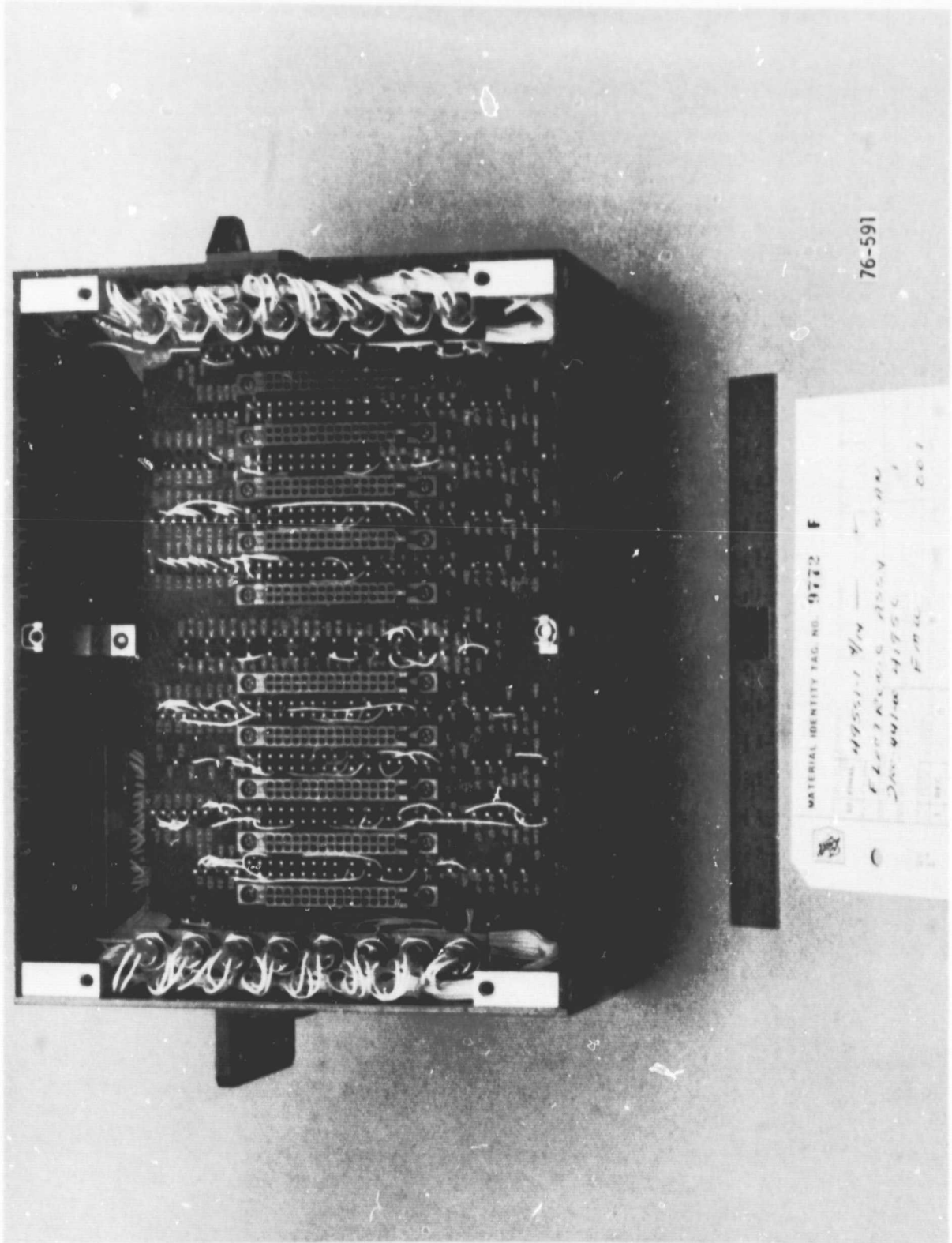


Figure 4-9 Scan Electronics Box



However, final adjustments are made during the combined tests of the two subsystems. The completely assembled Scan Electronics Subsystem mounted to the CZCS Protoflight is shown in Figure 4-10.

A functional block diagram of the scan drive and momentum compensator electronics is shown in Figure 4-11. The scanner motor, resolver and encoder are on the scan mirror shaft while the momentum compensator motor and resolver rotate on a common shaft with the compensator weight. In both cases, the motors are d.c. torquers commutated by the resolvers.

After the scan drive is turned on, the two systems operate for two minutes in an open loop mode. During this time, both are slowly brought up to speed maintaining compensation to within approximately 10 percent. After operating speed is achieved, the loops are closed and full compensation is achieved. Turn off is similar to turn on in that the system is put into open loop operation for a two minute ramp down.

Referring to Figure 4-11, all the relays are reset open at instrument power turn-on. A scanner ON command then applies 10 volts to the ramp generator and the one-shot multivibrator clocks the D type flip-flop closing relays  $K_1$  and  $K_2$ . This applies an R-C ramp voltage for two minutes to both the scanner and momentum compensator error inputs. The reference voltage applied to the momentum compensator by relay  $K_2$  provides an extra inertia offsetting torque boost during ramp up. As the ramp voltage builds up to a level consistent with scanner operating speed after approximately two minutes, the level detector circuitry clocks another D type flip-flop to close relays  $K_3$  and  $K_4$ . The other flip-flop is reset simultaneously to reopen relays  $K_1$  and  $K_2$ . The loops are closed and both systems rapidly achieve normal operating speed.

After the scan drive loop is closed the error signal comes from the phase detector filter-amplifier. The phase detector compares the 8,080 hertz reference clock with the frequency generated by the 1,000 line encoder and generates an error signal proportional to their phase difference. This error signal is summed and filtered with the reference voltage. After compensation by the lead-lag-lag amplifier, the error signal is modulated for the resolver. The

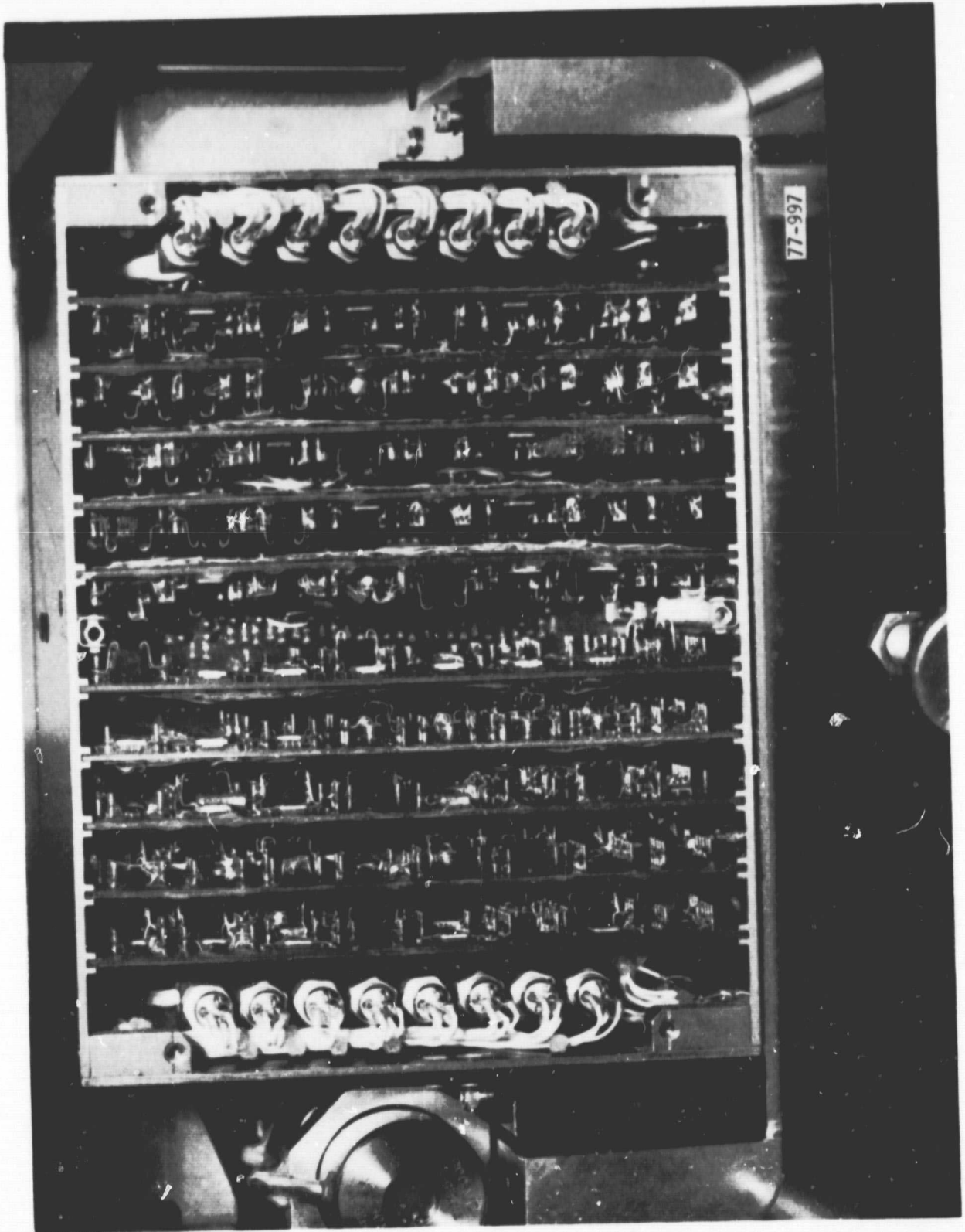


Figure 4-10 Scan Electronics Subsystem Assembled

ORIGINAL PAGE IS  
OF POOR QUALITY

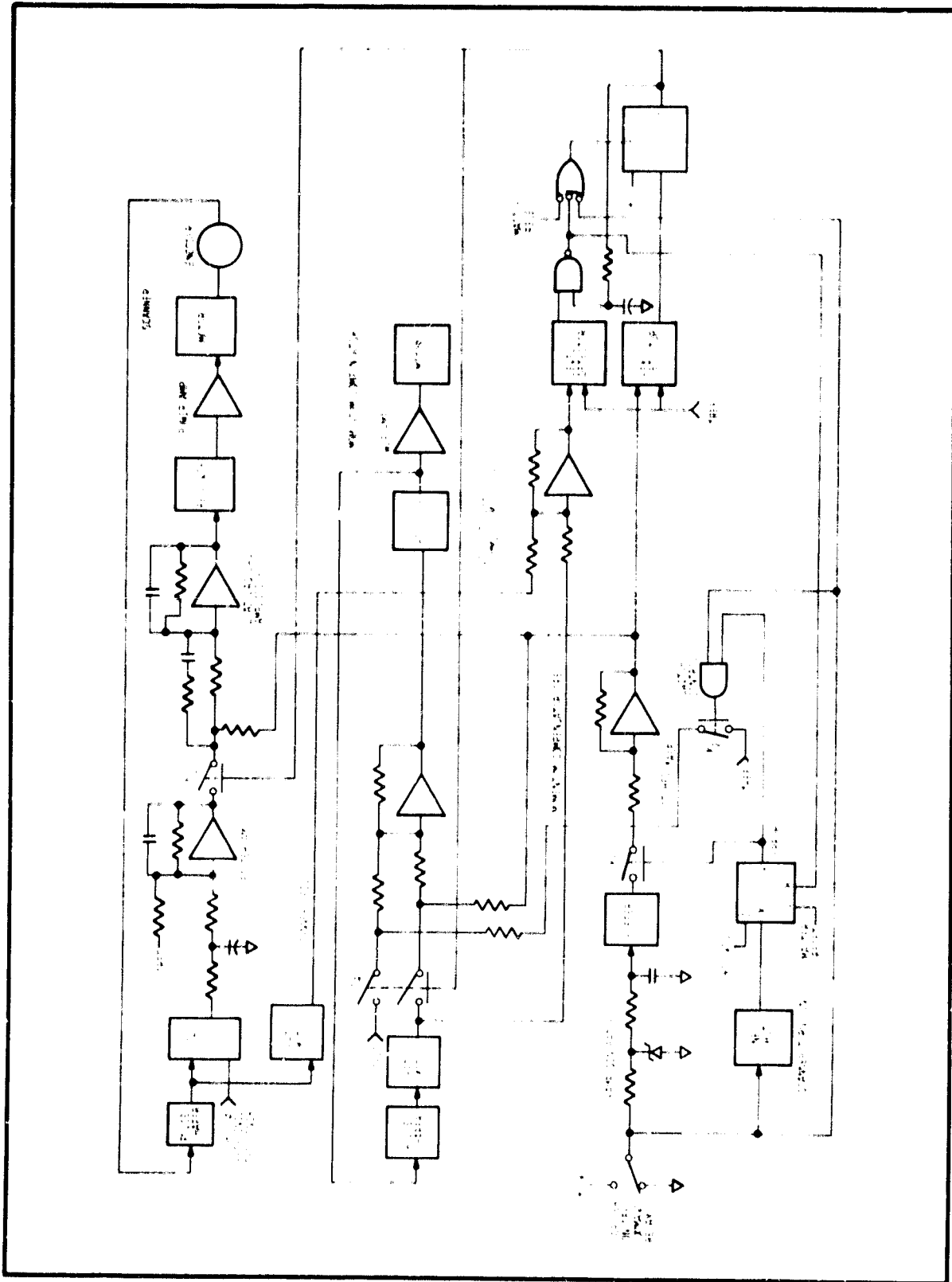


Figure 4-17 SCAN DRIVE/MOMENTUM COMPENSATOR FUNCTIONAL BLOCK DIAGRAM





resolver generates sine and cosine signals proportional to the error signal which are then amplified to drive the torquer motor.

The momentum compensator closed loop operation is similar. In this case, an error frequency is generated by the resolver and converted to a voltage level by the rate meter. The rate meter output is then summed with a voltage reference and amplified to drive the resolver. Another rate meter is used to generate the scanner speed telemetry level which is summed in the velocity error summing amplifier with the momentum compensator error signal. If either scanner drops off in velocity by more than approximately 15 percent, the level detector resets the flip-flop, opening  $K_3$  and  $K_4$ , and causes the two motors to coast to a stop. Relays  $K_3$  and  $K_4$  are also opened by the flip-flop being reset when a scanner off command is given. Relay  $K_1$  is again closed (but not  $K_2$ ) and the ramp generator discharges. The ramp down, like the ramp up, takes about two minutes.

#### 4.5 ANALOG ELECTRONICS SUBSYSTEM

The Analog Electronics Subsystem is a box containing seven circuit boards. Six of the boards provide amplification, bandpass (presampling) filtering, and d.c. restoration. The boards for the first four channels also have gain changing and offset circuitry while the Channel 6 board includes the preamplifier for the IR detector located in the radiative cooler. The seventh board includes circuitry for temperature monitoring and control of the radiative cooler. Each board operates independently and includes +12 volt and -12 volt regulators.

As shown in Figure 2-2, (Section 2) the analog electronics fits along the side of the spectrometer housing and actually attaches to the telescope plate of the Optical Subsystem. Figure 4-12 is a section of the Analog Electronics box while Figure 4-13 shows a typical circuit board. The analog signals and the telemetry levels are sent to the Main Electronics Subsystem for further processing.

Figure 4-14 illustrates the amplification technique used in Channels 1 through 4. This design allowed the preservation of the electrical bandwidth and minimizing of noise. If the feedback resistor,  $R_1$ , is made sufficiently small so

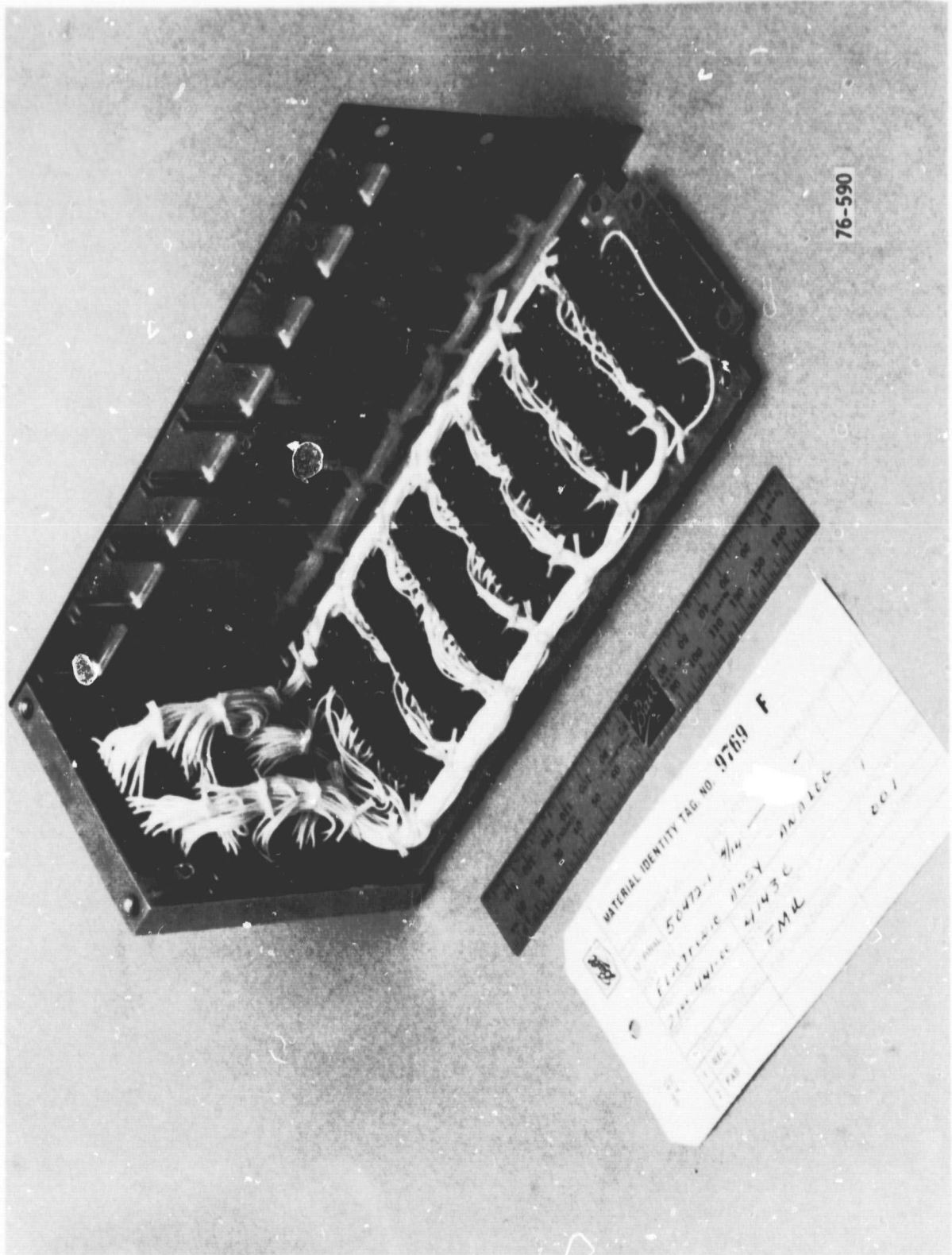


Figure 4-12 Analog Electronics Box

ORIGINAL PAGE IS  
OF POOR QUALITY

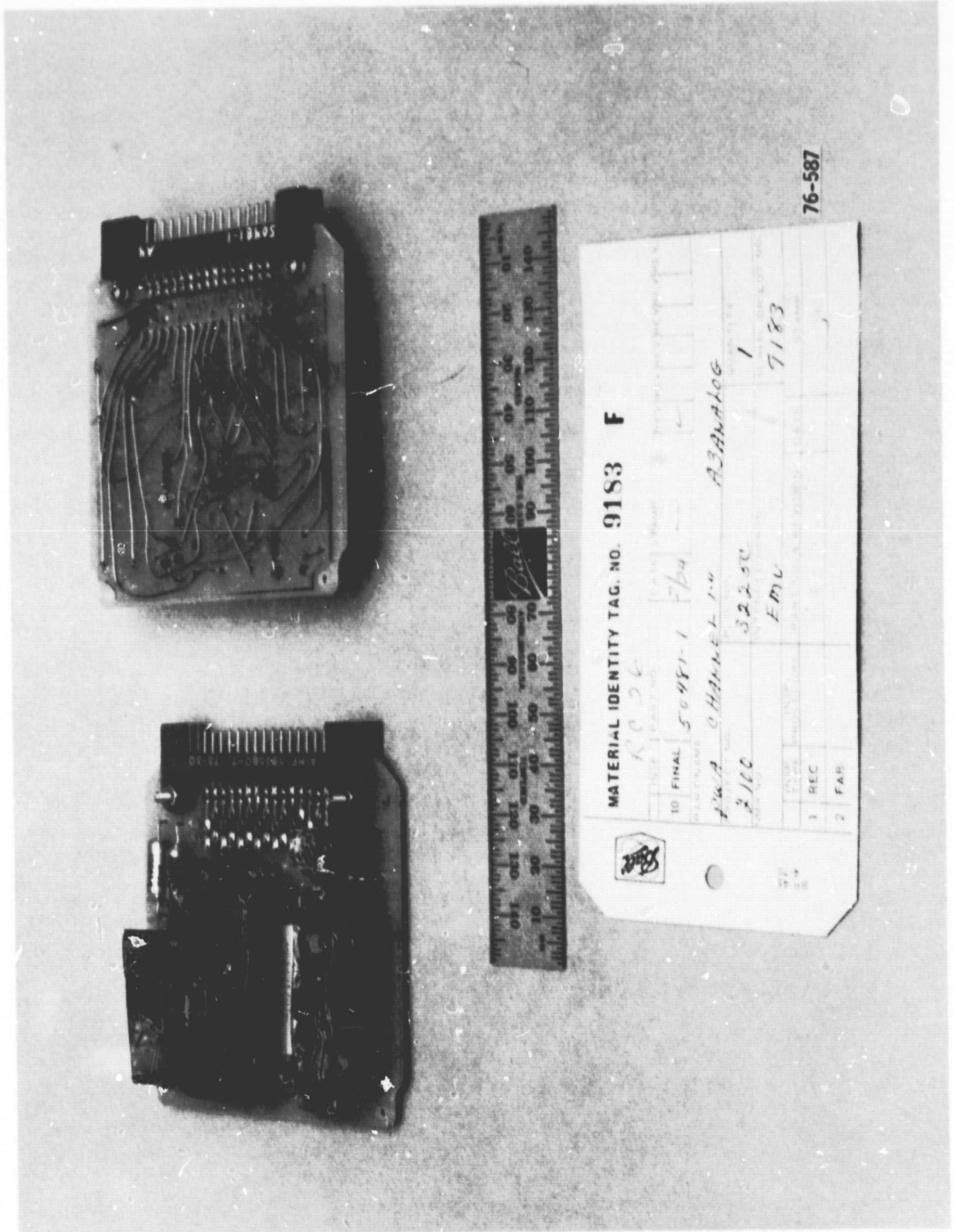


Figure 4-13 Typical Analog Electronics Circuit Board

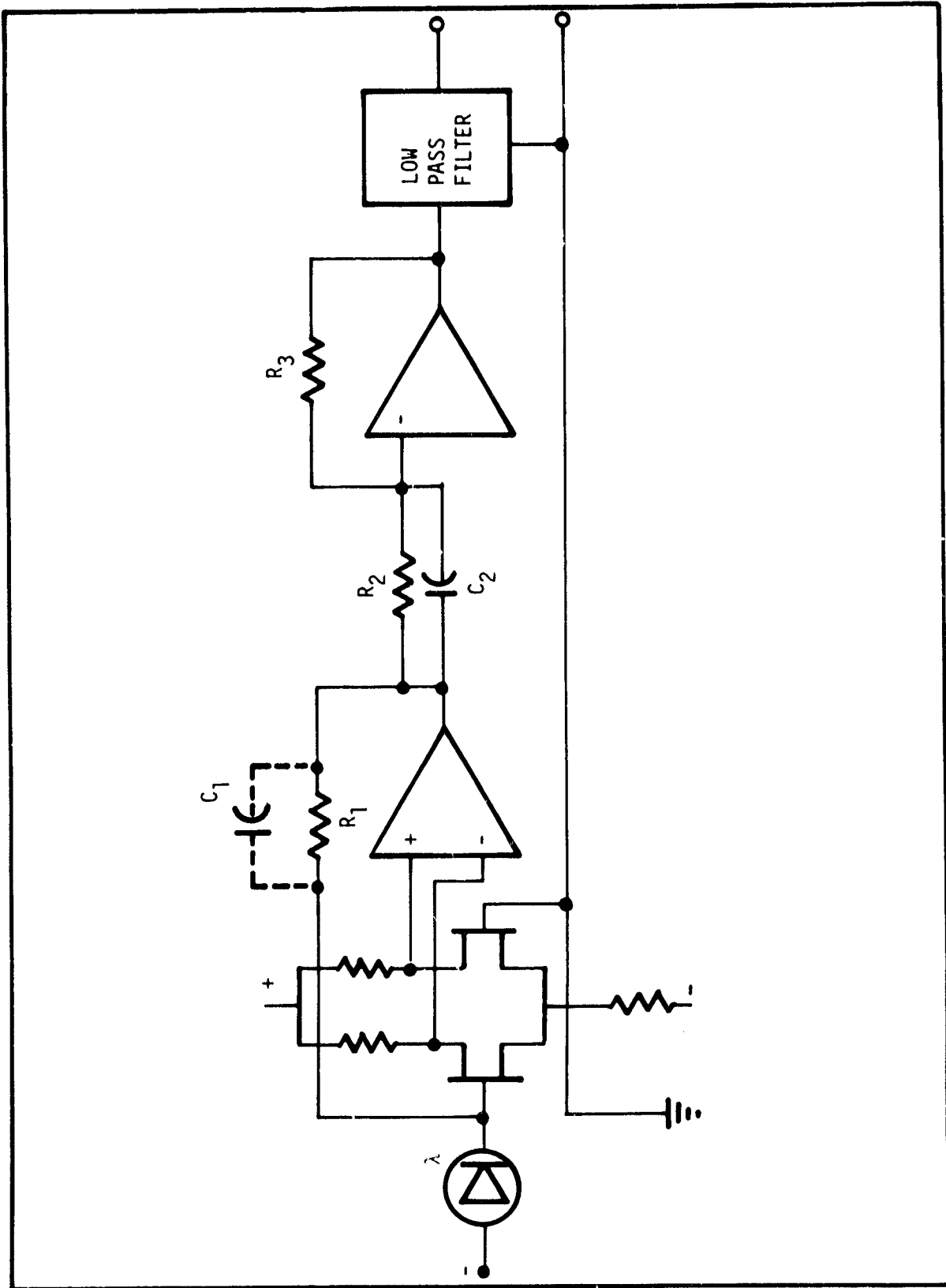


Figure 4-14 PEAKING PREAMPLIFICATION



there is no effect on the electrical bandpass due to the stray capacitance,  $C_1$ , the Johnson noise of the resistor predominates. If  $R_1$  is made sufficiently large so that its noise contribution is small, the preamp bandwidth is less than the required system bandwidth. The latter approach was taken. In the CZCS design  $R_1$  was made  $2 \times 10^8$  ohms and the high frequency falloff due to stray capacitance is compensated by  $R_2$  and  $C_2$ . With this design, detector capacitance also is a factor. Both detector leakage current (or dark current) and capacitance are proportional to detector area. The field lenses minimize the detector size thus minimizing the noise contributions of the detector capacitance and leakage current. This was one of the tradeoffs mentioned earlier and pitted the transmission loss of a lens against the detector noise components.

In Channel 5, the increased spectral bandwidth provided more signal (therefore more noise was acceptable) and the peaking preamplification technique was unnecessary. A smaller load resistance was used in Channel 5 without any problem. Effects due to quantization and photon noise are small. The SNR's for Channels 1 through 5 are shown as a function of scene radiance in Table 4-2.

Table 4-2  
SIGNAL TO NOISE RATIO AT MAXIMUM SCENE RADIANCES  
FOR A 60° SOLAR ZENITH ANGLE IN CHANNELS 1-5

<u>CHANNEL</u>	<u>SNR</u>	<u>SCENE RADIANCE</u> ( $\text{mw cm}^{-2}\text{sr}^{-1} \mu\text{m}^{-1}$ )
1	260	5.41
2	260	3.50
3	233	2.86
4	143	1.34
5	267	10.8



#### 4.6 MAIN ELECTRONICS SUBSYSTEM

The Main Electronics Subsystem is the nerve center of the CZCS. All spacecraft interfaces except for wiring to the scanner subsystem launch caging mechanism are located in the main electronics. It converts the spacecraft 1.6 Mhz clock and the 13.75 microsecond sampling line to the operational clock frequencies distributed to other subsystems. The main electronics also provides the power conversion and distribution function for the CZCS.

The main electronics box, shown as Figure 4-15, provides interconnections for fourteen circuit boards and a power supply assembly which fits in the long narrow space alongside the boards. The fourteen boards include circuitry for seven analog to digital converters (one for each channel and one for housekeeping telemetry), clock generators, timing circuits, commands and other interface functions. The unfolded power supply is shown in Figure 4-16. It is a self contained unit which can operate synchronized or unsynchronized. It provides  $\pm 16$  and  $\pm 15$  volts to analog and telemetry circuits, +10 volts and +5 volts for logic, +34 volts for the scanner, momentum compensator, cooler door, and calibration shutter motors, and +17 volts to the tilt drive motor. The main power relays and power line filters are also found in this assembly. A view of the Main Electronics Subsystem with the cover removed and completely assembled is provided by Figure 4-17.

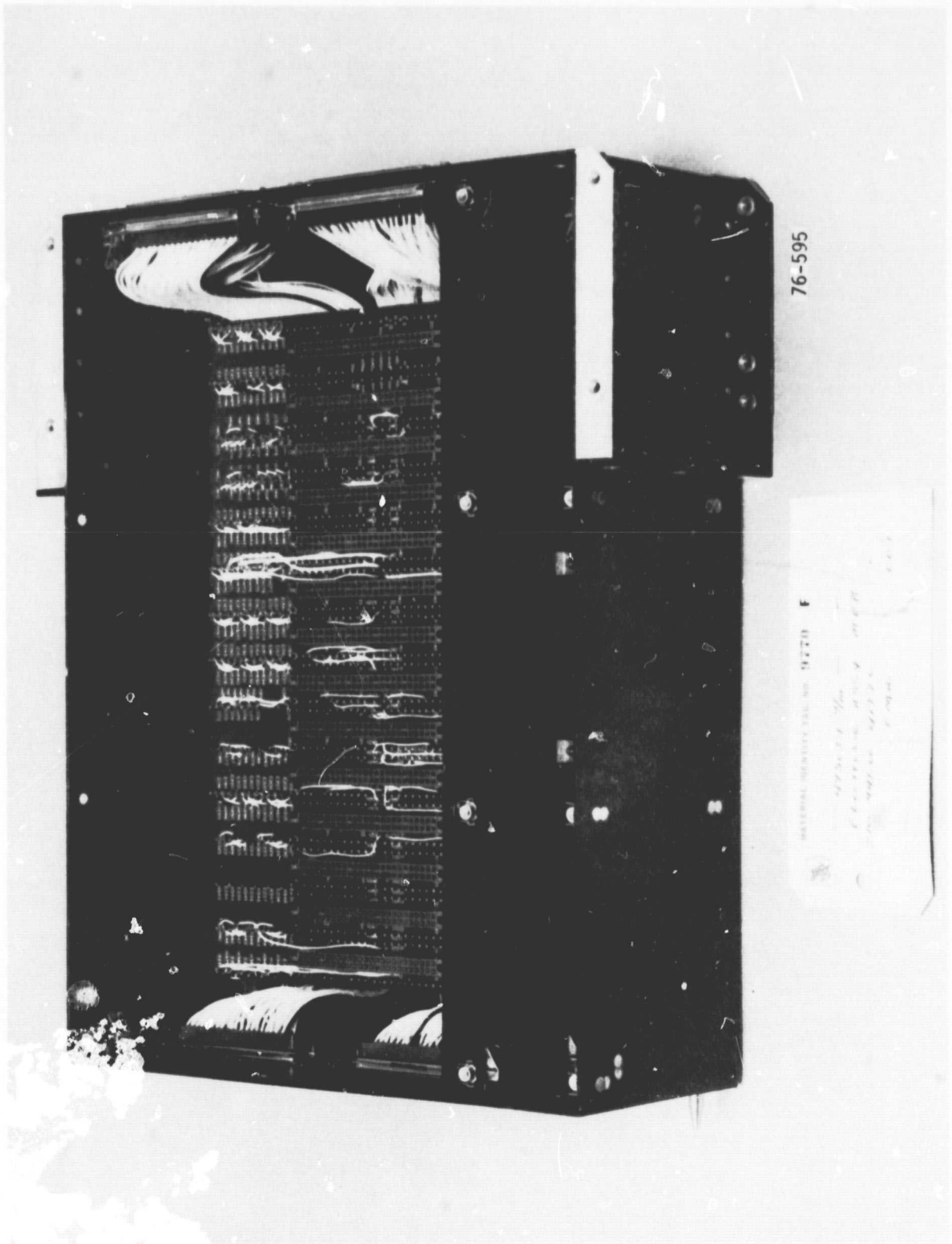


Figure 4-15 Main Electronics Box

ORIGINAL PAGE IS  
OF POOR QUALITY



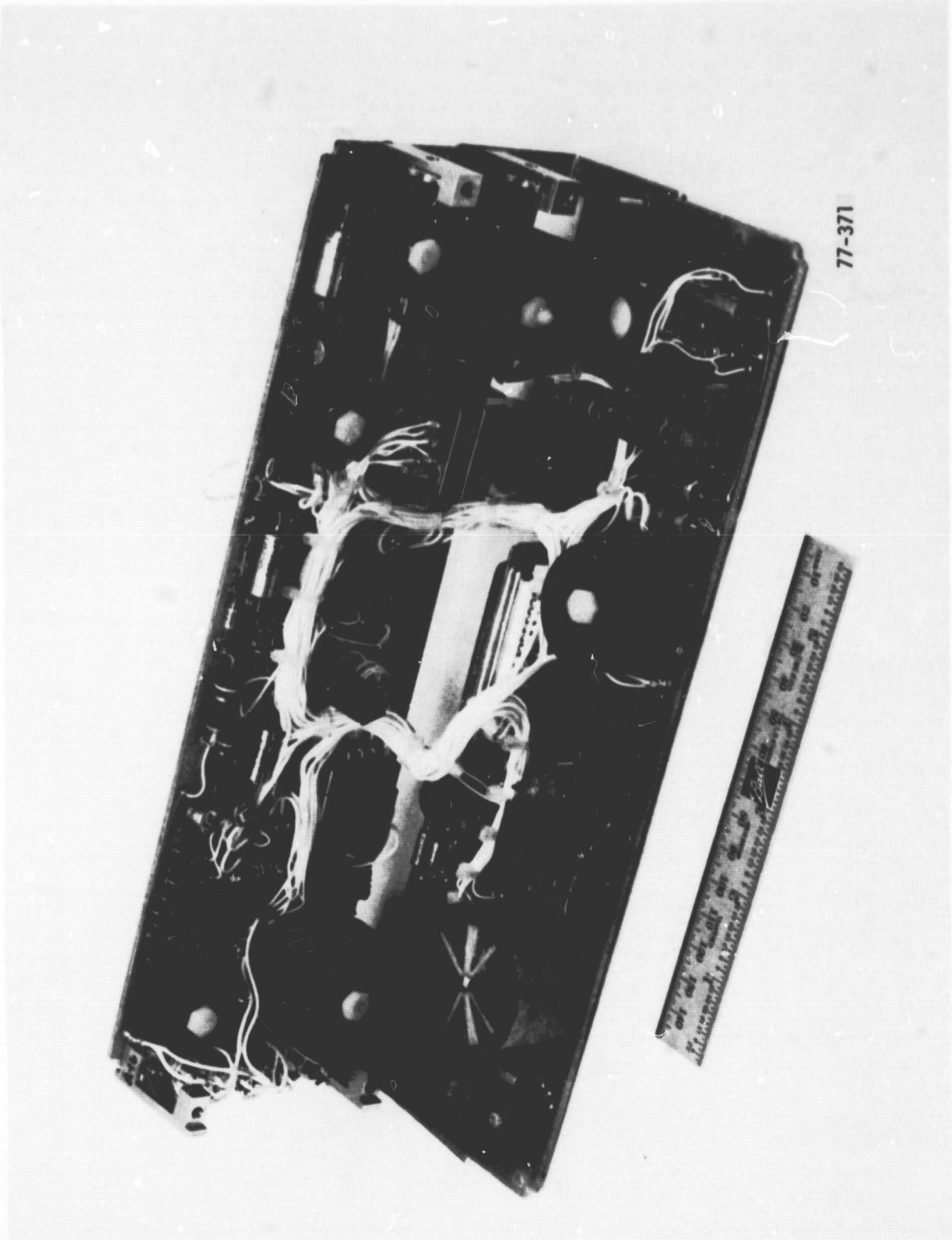


Figure 4-16 Power Supply Assembly



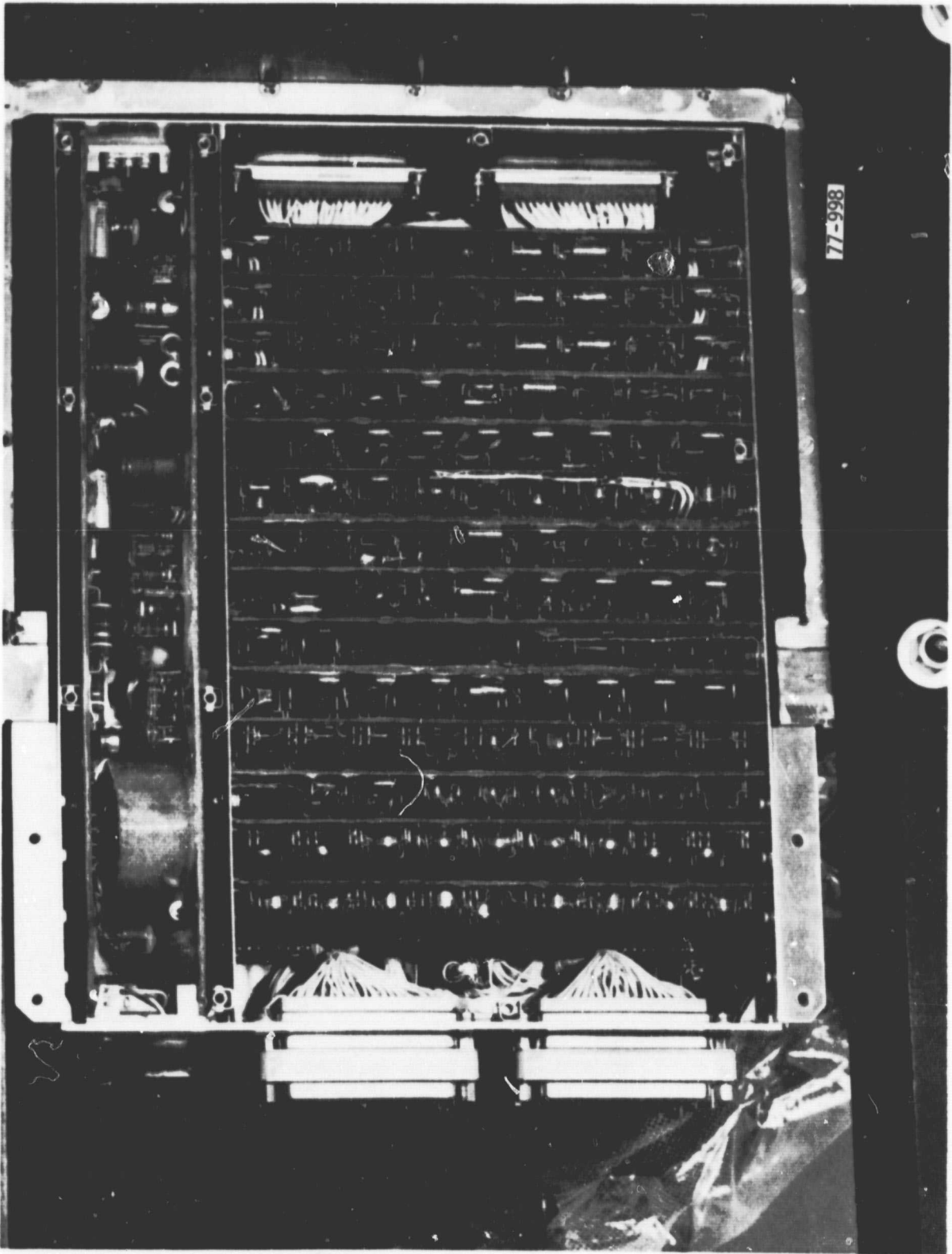


Figure 4-17 Main Electronics Box Assembled



## APPENDIX A SCIENCE BACKGROUND

### Mission Requirements

The mission of the Coastal Zone Color Scanner is the mapping of phytoplankton in the coastal areas of the ocean. Since plankton comprise the lowest level of the food chain for the organisms of the oceanic community, a high concentration of plankton indicates an area of high concentration of other organisms such as fish. Detection of plankton by remote sensing from the Nimbus 7 Observatory Satellite is possible because the plankton contain chlorophyll. As shown in Figure A-1,<sup>(1)</sup> chlorophyll found in the algae *Chlorella* have strong absorption in the measured reflectance characteristic at 450 and 675 nanometers. This reflectance characteristic along with many measurements made from low and high flying aircraft supported by surface truth measurements provided the basis for the selection of CZCS channels 1 and 4.

Unfortunately the atmosphere, particularly from Nimbus orbital altitude, presents a significant barrier to detection of ocean surface reflectance. This is illustrated by Figure A-2. The observatory sensor at the right top of the picture sees not only the source (the sun) reflected from the surface but also atmospheric and subsurface reflectance. Even on a clear day atmospheric scatter reflects a portion of the solar energy back toward the sensor and attenuates the surface reflected energy. Therefore, only a small portion of the energy sensed is caused by surface reflectance. This is demonstrated by Figure A-3, "Lear Jet Spectra at High and Low Altitudes".<sup>(2)</sup> The high altitude spectra is nearly identical to that seen from orbital altitude. The difference between the two spectra clearly demonstrates the difficulty involved in attempting to measure surface characteristics in the presence of the earth's atmosphere.

---

(1) Dr. Warren A. Hovis, "Measurements of Ocean Color," Significant Accomplishments in Sciences, NASA SP 312, November 1971, p. 25

(2) Dr. Warren A. Hovis, Michael L. Forman, Lamdin R. Blaine, "Detection of Ocean Color Changes from High Altitudes," GSFC X-652-73-371, November, 1973, p.6

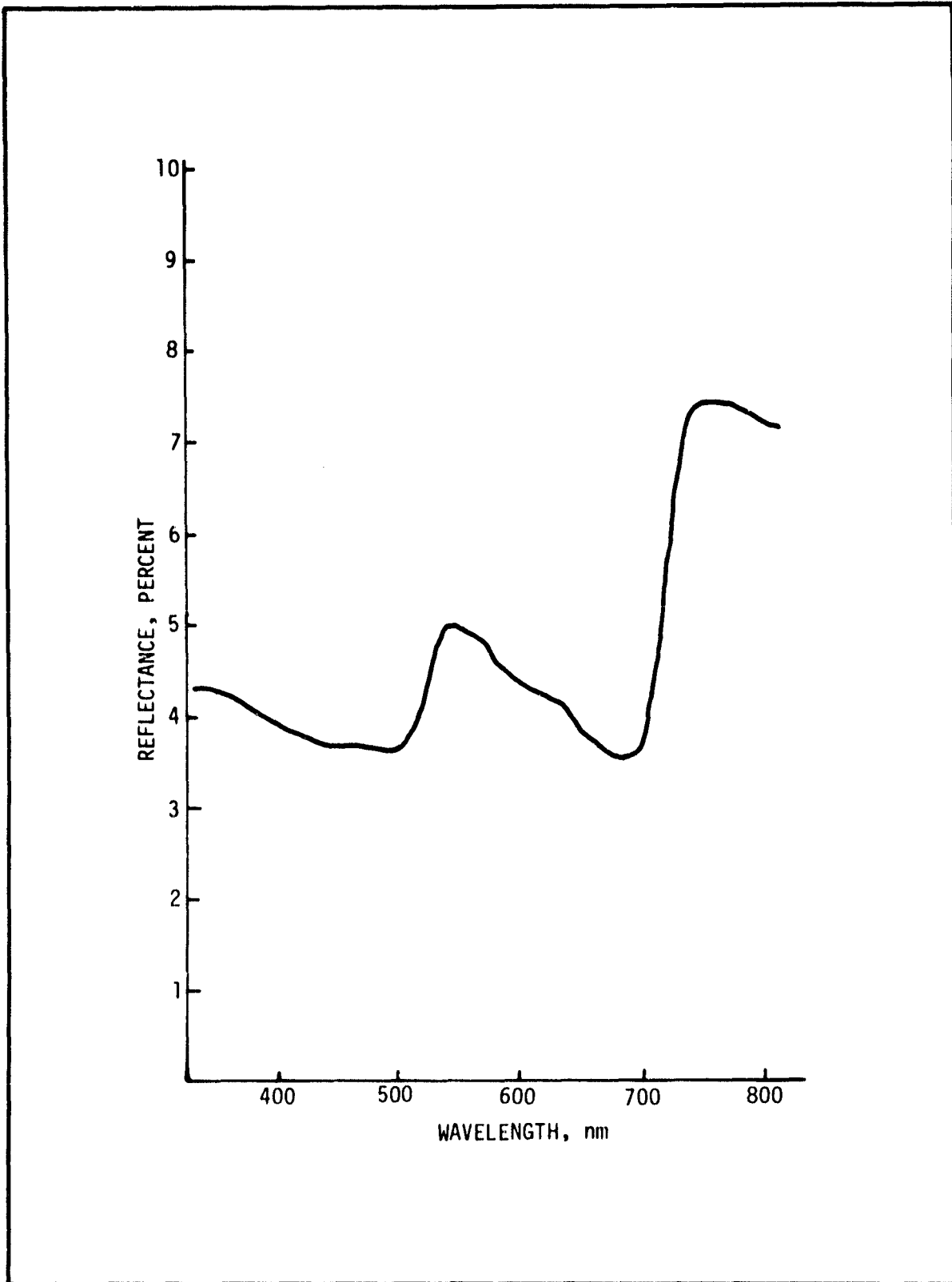


Figure A-1 Laboratory measured reflectance of Chlorella

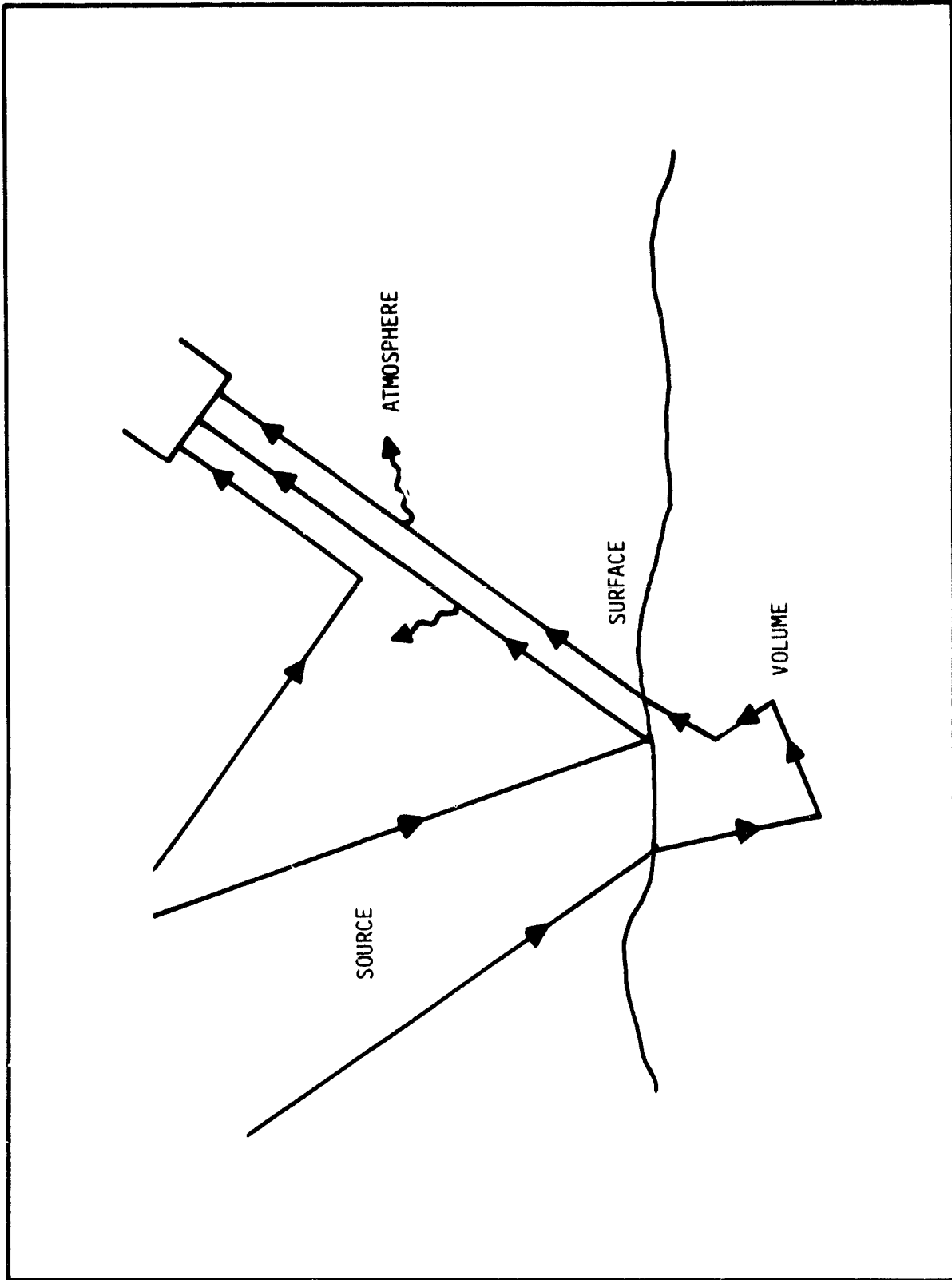


Figure A-2 ATMOSPHERIC AND ILLUMINATION EFFECTS INVOLVED IN ESTABLISHING THE EXPOSURE OF A BODY OF WATER

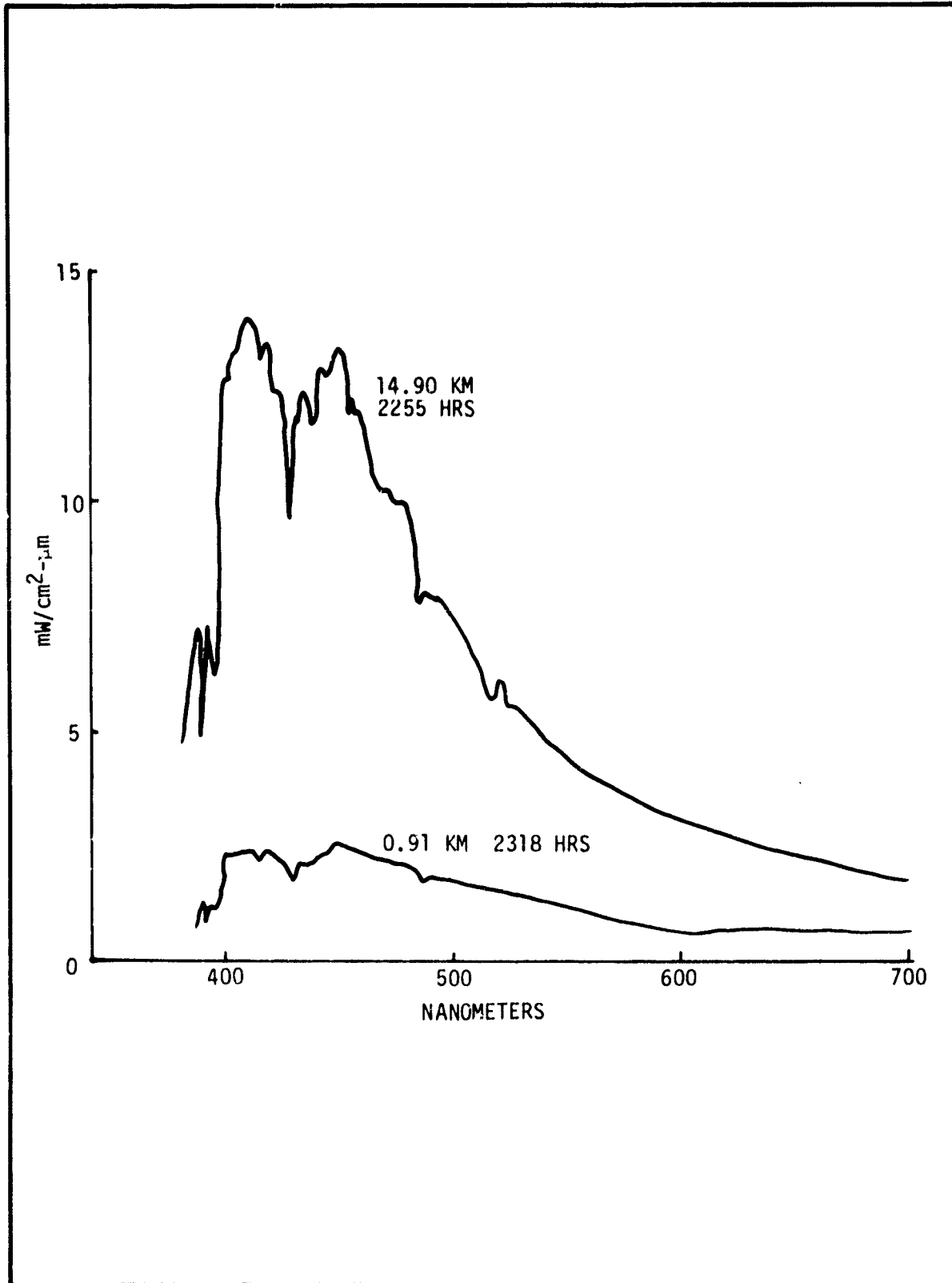


Figure A-3 LEAR JET SPECTRA AT HIGH AND LOW ALTITUDES



To reduce the atmospheric background effects, ratioing of data from spectral channels set at wavelengths of chlorophyll absorption and non-absorption was performed. These data were measured using an aircraft version of the CZCS having multiple channel selection capability. Figure A-4<sup>(3)</sup> shows five channels ratioed in four combinations along with surface truth data. High altitude spectral for two different chlorophyll concentrations are shown in Figure A-5<sup>(4)</sup>. This illustrates the spectrally selective radiance differences at 443 nm (channel 1) and 670 nm (channel 4). It also shows the lack of change at 520 nm (channel 2) and 550 nm (channel 3).

Channel 2 was set at 520 nm and is referred to as the correlation channel. It has been shown <sup>(5)</sup> that a linear relationship exists between the ratios of two spectral channel reflectances measured at the surface and measured through the atmosphere. The slope of this linear characteristic is a function of the optical depth and the solar zenith angle. The optical depth can be determined by a comparison of the various channel data with existing atmospheric models while the solar zenith angle is known for each orbit. The ratio of the surface reflectances for two channels can, therefore, be determined from the ratios of the reflectances measured through the atmosphere. The presence of chlorophyll in the water does not cause a change in the apparent reflectance of the correlation channel as it does in the chlorophyll sensitive channels. Therefore is a semi-logarithmic relationship between the ratio of the surface reflectances and the chlorophyll concentration (see Reference 5). Therefore, the chlorophyll concentration can be determined from the ratio of the surface reflectances.

---

(3) Ibid., p. 13

(4) Ibid., p. 19

(5) Dr. Robert J. Curran, "Ocean Color Determination Through a Scattering Atmosphere," Applied Optics, Vol. II, No. 8, August, 1972, pp. 1857-1866.

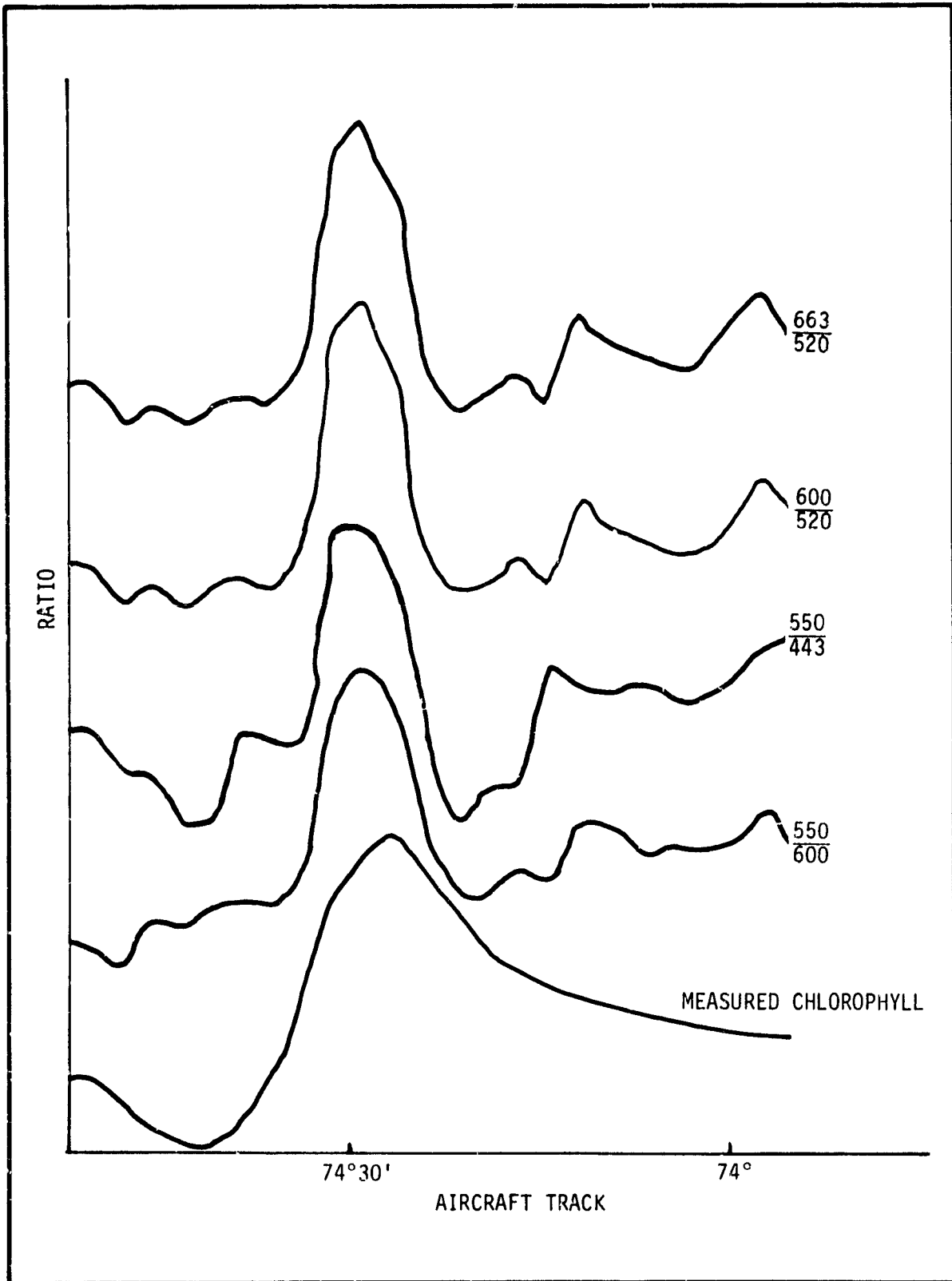


Figure A-4 RATIOS OF SELECTED WAVELENGTHS AND GROUND TRUTH VS. POSITION

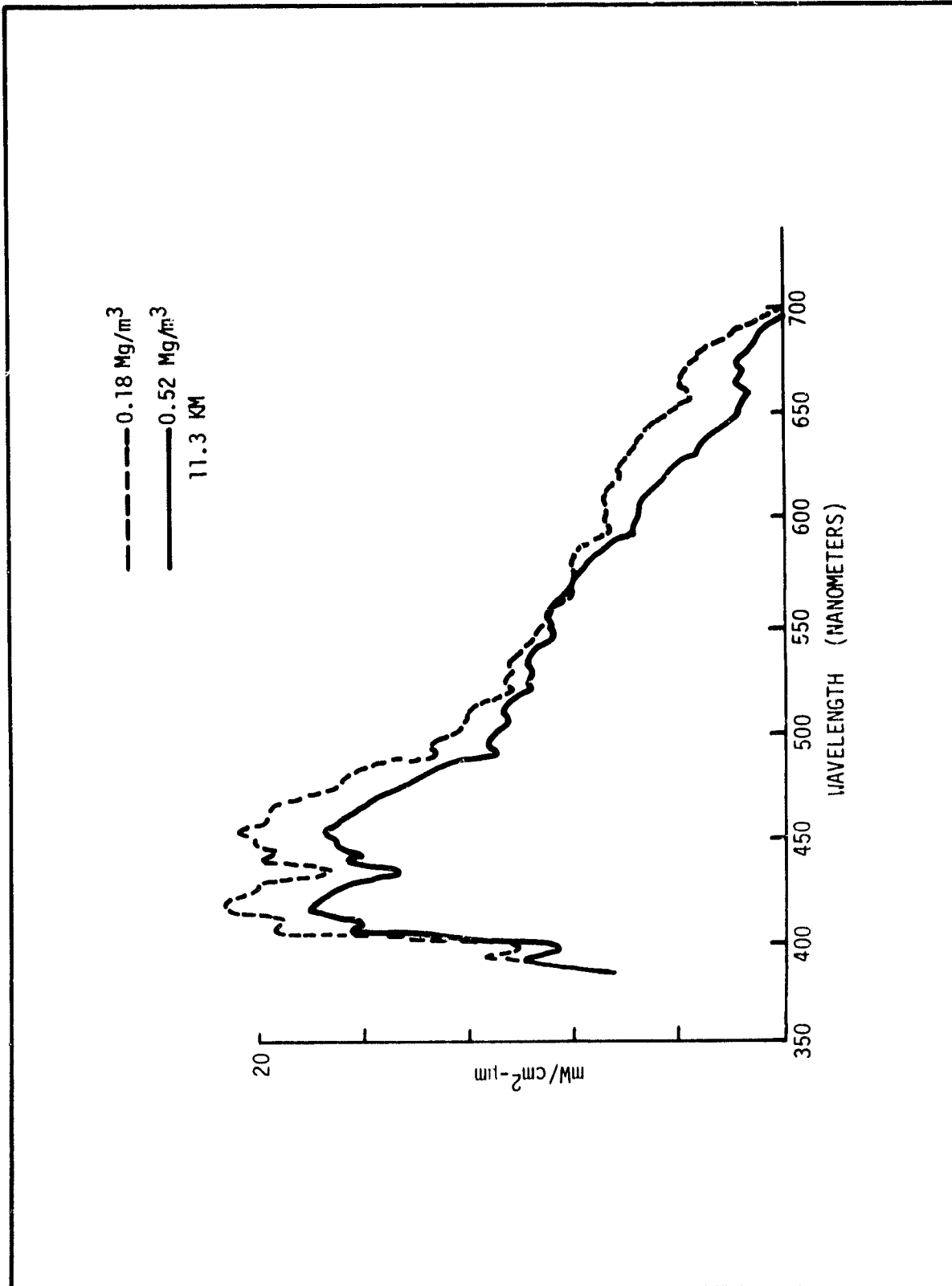


Figure A-5 HIGH ALTITUDE SPECTRA FOR TWG CHLOROPHYLL CONCENTRATIONS





In November 1974, measurements were made in the Gulf of Mexico to obtain correlation data from surface truth and aircraft measurement.<sup>(6)</sup> A preliminary algorithm was applied using two channels at a time. From spectral channels centered at 547 nm and 662 nm a best fit was obtained with the equation:

$$\frac{R662}{R547} = a + b \ln C \quad (1)$$

were  $R662$  = unenhanced radiance at 662 nm  
 $R547$  = unenhanced radiance at 547 nm  
 $a = 0.309$   
 $b = 0.0166$   
 $c$  = chlorophyll in  $Mg/M^3$

From the data obtained from the two channels the chlorophyll concentration may be calculated from the equation:

$$c = e^{\frac{1}{b} \left( \frac{R662}{R547} - a \right)} \quad (2)$$

Figure A-6 is a comparison of the calculated values for chlorophyll concentration compared to surface truth measurements. This was the first attempt to applying an algorithm to imagery. The algorithm will be further refined to utilize more than two channels

The third channel is set at 550 nm for the measurement of gelbstoffe (yellow stuff) which is the sediment found in estuarine or coastal waters. This channel is ratioed with one of the other channels for determination of sediment density. Tests performed with the airborne instrument over the Hudson River plume showed a remarkable correlation between surface truth and calculated measurements.

---

(6) W.A. Hovis, and K.C. Leung, "Remote Sensing of Ocean Color," Optical Engineering, Vol. 16, No. 2, March-April, 1977.

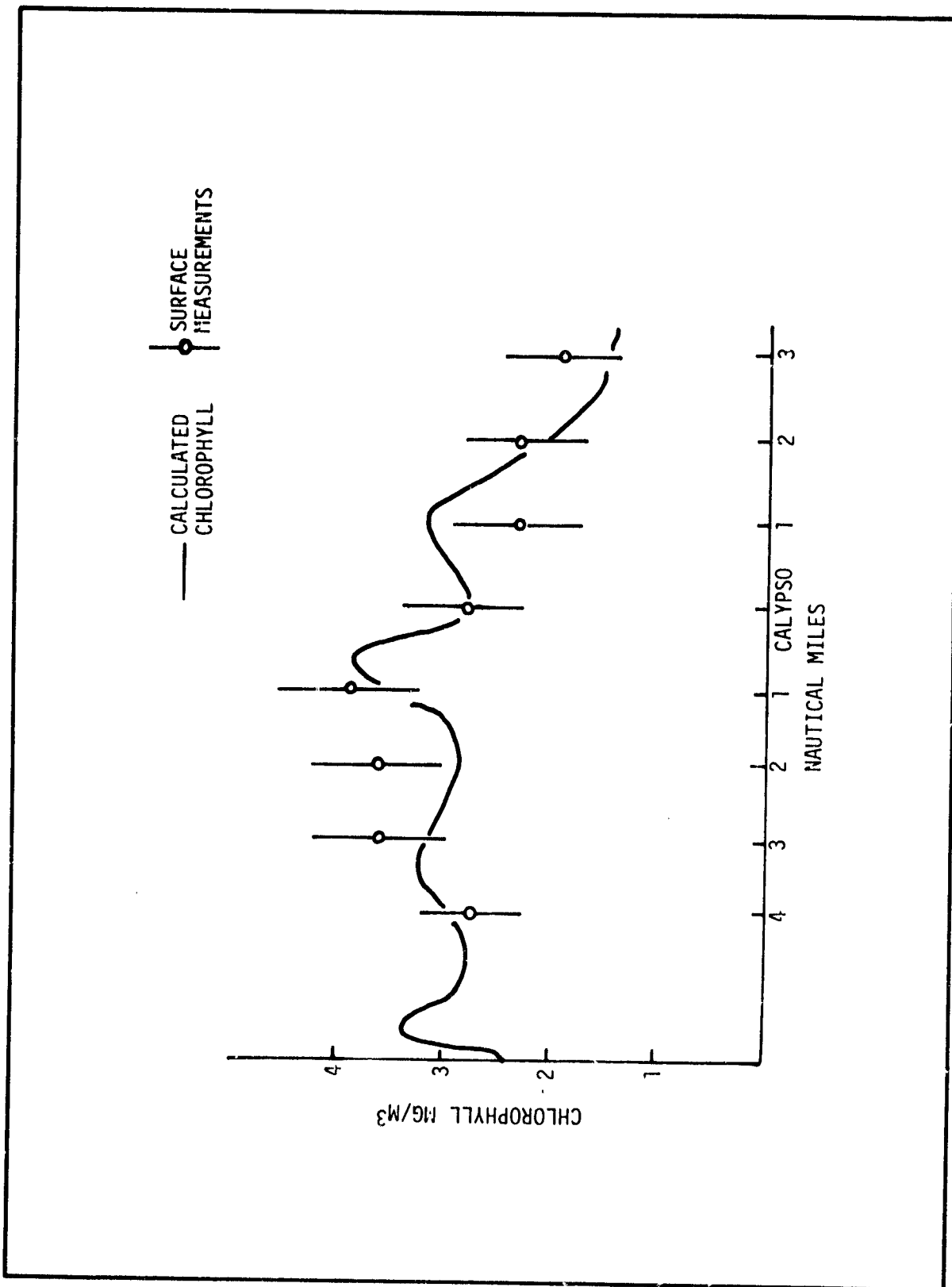


Figure A-6 CALCULATED VS. MEASURED CHLOROPHYLL CONCENTRATION, GULF OF MEXICO



Measurements of the gelbstoffe concentrations also provide relative salinity information through the use of established models. The fifth channel selected for the CZCS is the same as one of the Landsat Multispectral Scanner channels. Spectrally, it extends from 700 to 800 nm and is used to detect surface vegetation. With the high spectral reflectance of water plants in the near-IR, channel five provides an indication of the presence of vegetation which could otherwise contaminate channels two and three. This channel also provides another data point for determination of optical depth.

The sixth CZCS channel is included to measure surface temperature in the 10.5 to 12.5 micrometer atmospheric "window." Cold water upwellings frequently provide the nutrients necessary for plankton "blooms." Figure A-7<sup>(7)</sup> illustrates this relationship between the cold water upwellings and chlorophyll (phytoplankton) concentrations. Additional uses for channel six are mapping of sea ice and nighttime cloud mapping. As a review, the six spectral channels of the CZCS and their intended uses are as listed below.

<u>Channel No.</u>	<u>Spectral Interval (<math>\mu\text{m}</math>)</u>	<u>Purpose</u>
1	0.433 - 0.453	Chlorophyll
2	0.510 - 0.530	Correlation
3	0.540 - 0.560	Yellow Stuff
4	0.660 - 0.680	Chlorophyll
5	0.700 - 0.800	Surface Vegetation
6	10.5 - 12.5	Surface Temperature

A relatively large percentage of the radiance incident on the orbiting sensor is polarized. In general, the greater the atmospheric attenuation and scatter, the more polarized the light becomes. Polarization of scene radiance greater

---

(7) John C. Arvesen, John P. Millard, Ellen C. Weaver, "Remote Sensing of Chlorophyll and Temperature in Marine and Fresh Waters", NASA, Ames Research Center, Document No. 225, Revised March, 1970.

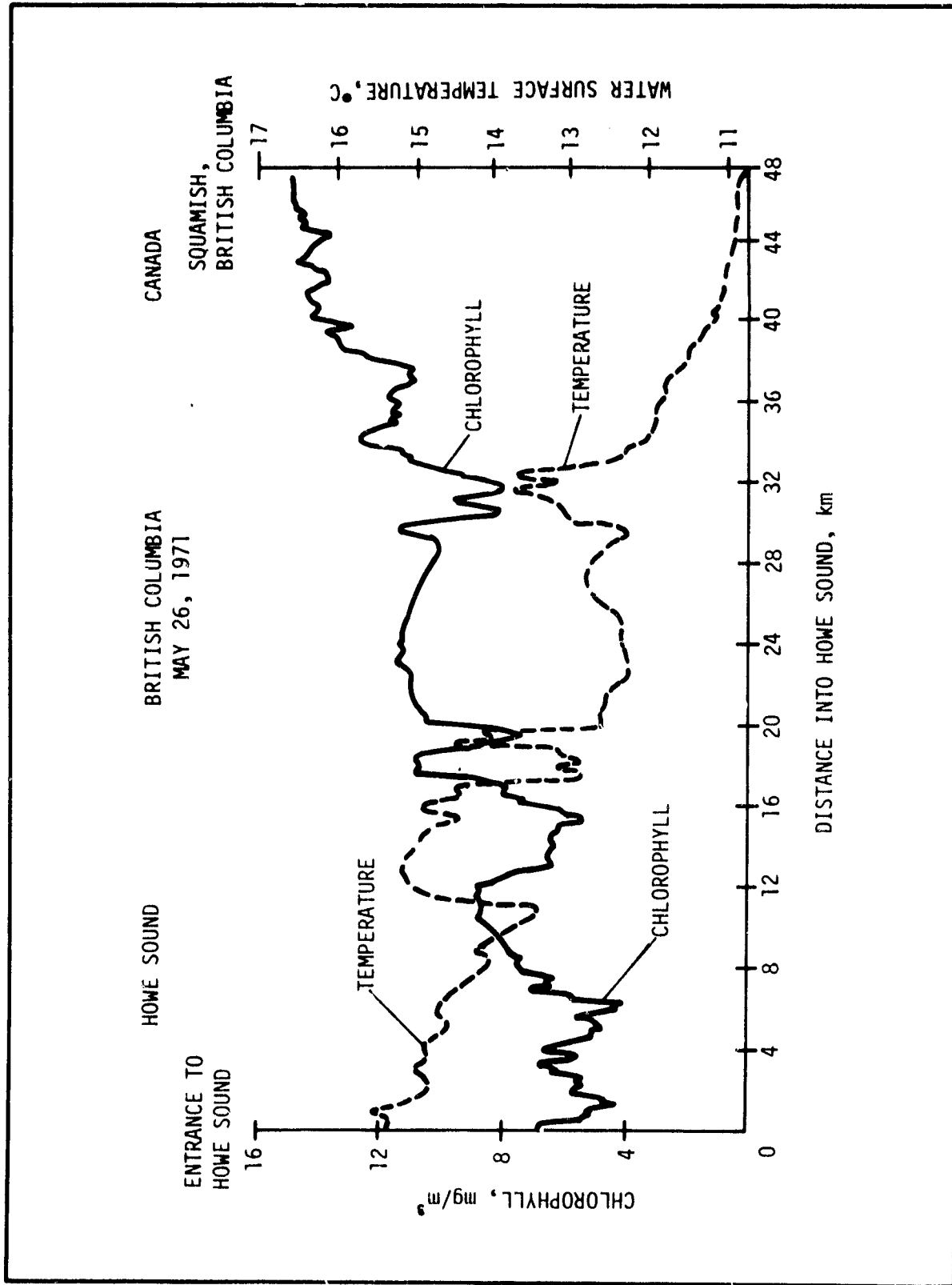


Fig. A-7 CHLOROPHYLL AND TEMPERATURE CORRELATION IN HOWE SOUND British Columbia, Canada on May 26, 1971.



than 50% has been observed in "blue" end of the solar spectra. This being the case, it is necessary that the sensor have little, if any, sensitivity to the polarization orientation of the incoming energy. A specification of 2% or less sensitivity to incoming energy polarized to 100% has been required. In Section 3.4, the system design to meet this requirement is addressed. The other "natural" problem is sun glitter or glint. This is a direct specular reflection of the sun from the wave facets of the ocean surface which obscures the true color of the water. Glint intensity diminishes rapidly when the sensor is aligned to view the surface in a direction away from the sun. The sensor viewing direction shown in Figure A-2 then is not ideal. A requirement was imposed, then, to make the scan tiltable  $\pm 20^\circ$  along the spacecraft ground track in  $2^\circ$  increments. This allows selection of an optimum viewing angle which is dependent on the solar zenith angle for any orbit.

System level testing indicates that the instrument design has achieved a high degree of success in meeting the scientific requirements.